Extending the knowledge on performance monitoring in obsessive-compulsive disorder: Insights gained by electrophysiological recordings and deep brain stimulation.

Inaugural Dissertation

zur

Erlangung des Doktorgrades
philosophiae doctor (PhD) in Health Sciences
der Medizinischen Fakultät
der Universität zu Köln

vorgelegt von

Elena Sildatke
aus Mykolayiv, Ukraine

Universitäts- und Stadtbibliothek Köln

2022

Betreuer*in:	Prof. Dr. Jens Kuhn
Gutachter*in:	Prof. Dr. Christian Grefkes
	PD Dr. Haidar Dafsari
	Prof. Dr. Silvia Daun

Datum der Mündlichen Prüfung: 07.07.2022

Table of contents

List of abbreviations

ALIC	Anterior limb of internal capsule
CRN	Correct-related negativity
CSTC	Cortico-striato-thalamo-cortical
DBS	Deep brain stimulation
dwPLI	Debiased weighted Phase-Lag Index
EEG	Electroencephalography
ERN	Error-related negativity
ERP	Event-related potential
FCz	Fronto-central electrode
FDR	False-Discovery Rate
GPi	Globus pallidus interna
IC	Independent component
ICA	Independent Component Analysis
LFP	Local-field potential
MFC	Mediofrontal cortex
NAc	Nucleus accumbens
OCD	Obsessive-compulsive disorder
RT	Reaction time
SNr	Substantia nigra
STN	Nucleus subthalamicus
THS	Tiefe Hirnstimulation
Y-BOCS	Yale-Brown Obsessive Compulsive scale

Summary

Obsessive-compulsive disorder (OCD) is characterized by alterations in frontostriatal circuits and associated impairments in performance monitoring. The overactivity of the performance monitoring system is reflected by enhanced electrophysiological correlates during decision conflict (conflict-theta) and error processing (error-theta and error-related negativity, ERN). Besides the mediofrontal cortex, composing the source of these correlates, further brain structures are fundamentally involved in these cognitive processes. Particularly, the anterior limb of internal capsule (ALIC) and nucleus accumbens (NAc) are not only involved in performance monitoring but show partially also altered activity in OCD. Despite the importance of ALIC/NAc in performance monitoring observation of its electrophysiological activity during decision conflict and error processing are limited. Notably, ALIC/NAc has been established as target region for deep brain stimulation (DBS) for treatment resistant OCD and has proved to be clinically effective. Although, it is still unknown whether stimulation of the ALIC/NAc affects the aforementioned cortical correlates.

In the first part of the present dissertation, electrophysiological activity during decision conflict and error processing from the cortex and the ALIC/NAc (by means of local-filed potentials, LFP) was investigated in patients with OCD (**LFP-study**). As expected, previous findings were successfully replicated cortical correlates of decision conflict (conflict-theta) and error processing (error-theta and ERN) were observed. Additionally, it was hypothesized that LFPs from the ALIC/NAc also comprises correlates of decision conflict (LFP-conflict-theta) and error processing (LFP-error-theta and LFP-ERN). Indeed, all three performance monitoring modulations were observed in the ALIC/NAc. Accordingly, ALIC/NAc seems to be involved in processes associated with monitoring of decision conflict and performance errors. Presumably, it provides the signal for the need of increased cognitive control to resolve the conflict and of behavioral adaptation to improve performance, respectively. Although, it was expected to find increased frontostriatal connectivity during decision conflict and error monitoring, this was not confirmed. Putatively, this could be explained by increased connectivity between both structures irrespective of cognitive control demands in OCD. Finally, possible interrelations between striatal correlates and symptom severity or symptom improvement by DBS in OCD were explored. Our results indicated an association of patients who exhibited smaller error signals (LFP-error-theta and LFP-ERN) with lesser symptom severity and with greater DBS efficacy. This links ALIC/NAc performance monitoring modulations to OCD symptomatology, possibly reflecting hyperactive performance monitoring, and connect this to attenuated response to DBS.

In the second part of the present dissertation, the modulatory effect of DBS on cortical correlates of decision conflict (conflict-theta) and error processing (ERN) was investigated by comparing the correlates from pre-DBS state with stimulation on and stimulation off (**Stimulation-study**). It was hypothesized that acute DBS reduces conflict-theta and the ERN and that these effects would rebound after cessation of stimulation. In line with our hypotheses, the correlates were decreased by acute stimulation, indicating DBS-induced reduction of the pathologically overactive performance monitoring system. Contrary to our hypotheses, the rebound effect after cessation of stimulation was not observed for conflict-theta but at trend level for the ERN. Likely, DBS has only acute and no long-term effects on the performance monitoring system, which might become clearer by extending the stimulation off phase. Finally, possible interrelations between clinical efficacy of DBS with pre-DBS conflict-theta and the ERN and their changes through stimulation were explored. Our results associated patients who exhibited smaller pre-DBS ERN with greater DBS efficacy.

In conclusion, this dissertation provides new insights on electrophysiological correlates of performance monitoring in OCD derived from ALIC/NAc and on the modulation of their cortical pendants by DBS. Further investigations, particularly involving long-term acquisition of LFPs, are required to further characterize ALIC/NAc activity during performance monitoring and its association with the pathophysiology of DBS. Also, additional studies are needed to confirm the interrelation between electrophysiological correlates and clinical parameters with regard to clinical applications in the future. Particularly, it should be further explored whether increased cortical and striatal error signals point toward a hyperactive performance monitoring system and are also related to attenuated clinical efficacy.

Zusammenfassung

Die Zwangsstörung ist charakterisiert durch Veränderungen der fronto-striatalen Regelkreise und damit verbundener Handlungsüberwachung. Die Überaktivität des Handlungsüberwachungs-Systems wird reflektiert durch erhöhte elektrophysiologische Korrelate während des Entscheidungskonfliktes (Konflikt-Theta) und der Fehlerverarbeitung (Fehler-Theta und Fehler-assoziierte Negativität, engl. error-related negativity, ERN). Neben dem medialen frontalen Kortex, welcher die Quelle dieser Korrelate darstellt, sind weitere Hirnareale in diese kognitiven Prozesse grundlegend involviert. Insbesondere sind der vordere Schenkel der inneren Kapsel (engl. anterior limb of internal capsule, ALIC) und der Nukleus accumbens (NAc) nicht nur in die Handlungsüberwachung involviert, sondern weisen bei der Zwangsstörung außerdem veränderte Aktivität auf. Trotz der Wichtigkeit dieser Strukturen für die Handlungsüberwachung gibt es nur wenige Beobachtungen der elektrophysiologischen Aktivität von ALIC/NAc während des Entscheidungskonflikts und der Fehlerverarbeitung. Beachtenswerterweise hat sich die tiefe Hirnstimulation (THS) in der Zielstruktur ALIC/NAc zur Behandlung therapieresistenter Zwangsstörung als klinisch effektiv erwiesen und etabliert. Dennoch sind die Auswirkungen der Stimulation des ALIC/NAc auf die zuvor erwähnten kortikalen Korrelate bislang unklar.

Im ersten Teil dieser Dissertation wurde die elektrophysiologische Aktivität während des Entscheidungskonflikts und der Fehlerverarbeitung im Kortex und im ALIC/NAc (mithilfe lokaler Feldpotentiale, LFP) in Patienten mit einer Zwangsstörung untersucht (**LFP-Studie**). Wie erwartet, wurden die vorhergehenden Befunde erfolgreich repliziert und kortikale Korrelate des Entscheidungskonfliktes (Konflikt-Theta) und der Fehlerverarbeitung (Fehler-Theta und ERN) gefunden. Zusätzlich wurde die Hypothese aufgestellt, dass LFPs im ALIC/NAc ebenfalls Korrelate des Entscheidungskonfliktes (LFP-Konflikt-Theta) und der Fehlerverarbeitung (LFP-Fehler-Theta und LFP- ERN) aufweisen. Tatsächlich konnten alle drei Modulationen der Handlungsüberwachung im ALIC/NAc beobachtet werden. Demnach scheint ALIC/NAc in die Überwachungsprozesse während des Entscheidungskonfliktes und der Performance-Fehler involviert zu sein. Vermutlich vermittelt es die Notwendigkeit eines erhöhten kognitiven Kontrollbedarfs zur Lösung des Konflikts sowie zur Verhaltungsanpassung zwecks verbesserter Performanz. Die von uns erwartete Erhöhung der fronto-striatalen Konnektivität während des Entscheidungskonflikts und der Fehlerverarbeitung konnte nicht bestätigt werden. Möglicherweise kann dies dadurch erklärt werden, dass die Konnektivität zwischen der beiden Strukturen ungeachtet des kognitiven Kontrollbedarfs bei der Zwangsstörung erhöht ist. Schließlich wurden mögliche

Zusammenhänge zwischen den striatalen Korrelaten und der Symptomschwere oder Symptomreduktion durch THS bei der Zwangsstörung exploriert. Unsere Ergebnisse deuteten auf eine Assoziation zwischen Patienten mit kleineren Fehlersignalen (LFP-Fehler-Theta und LFP-ERN) und geringerer Symptomschwere sowie größerer Effizienz durch THS. Einerseits stellten unsere Ergebnisse einen Zusammenhang zwischen den Modulationen der Handlungsüberwachung im ALIC/NAc und der Symptomatik bei der Zwangsstörung her und reflektieren womöglich das hyperaktive Handlungsüberwachungs-System. Andererseits zeigten sie eine Assoziation zwischen den ALIC/NAc Modulationen und abgeschwächter Reaktion auf die THS.

Im zweiten Teil der vorliegenden Dissertation wurde der modulatorische Effekt der THS auf kortikale Korrelate des Entscheidungskonflikts (Konflikt-Theta) und der Fehlerverarbeitung (ERN) untersucht. Hierfür wurden die Korrelate während des pre-THS Zustands, bei eingeschalteter Stimulation sowie bei ausgeschalteter Stimulation verglichen (**Stimulation-Studie**). Es wurde vermutet, dass akute THS die Korrelate (Konflikt-Theta und ERN) reduziert und dass dieser Effekt nach Ausschalten der Stimulation wieder verschwindet. Unseren Annahmen entsprechend, wurden verringerte Korrelate bei akuter Stimulation beobachtet, was auf eine THS-induzierte Reduktion des pathologisch überaktiven Handlungsüberwachungs-Systems deutet. Abweichend von unseren Annahmen, konnte nach Ausschalten der Stimulation kein Wiederanstieg zum pre-THS-Zustand bei Konflikt-Theta, und nur eine Tendenz bei der ERN beobachtet werden. Möglicherweise hat die THS lediglich einen akuten und keinen Langzeiteffekt auf das Handlungsüberwachungs-System, was möglicherweise erst durch längere Ausschaltphasen deutlich werden könnte. Schließlich wurden mögliche Zusammenhänge zwischen klinischer Effektivität der THS und der pre-THS Konflikt-Theta und ERN sowie deren Veränderungen durch Stimulation exploriert. Unsere Ergebnisse zeigten eine Assoziation zwischen Patienten, die eine kleinere pre-THS ERN aufwiesen mit größerer THS Effektivität.

Zusammengefasst liefert diese Dissertation neue Erkenntnisse zu elektrophysiologischen Korrelaten der Handlungsüberwachung im ALIC/NAc bei der Zwangsstörung sowie zur Modulation deren kortikaler Pendants durch THS. Zur weiteren Charakterisierung der ALIC/NAc Aktivität während der Handlungsüberwachung sowie deren Zusammenhang mit der Pathophysiologie von THS sind zusätzliche Untersuchungen erforderlich. Von besonderem Nutzen wären hierbei Langzeiterhebungen der LFPs. Ferner sind weitere Studien notwendig, um die Zusammenhänge zwischen elektrophysiologischen Korrelaten und klinischen Parametern hinsichtlich der zukünftigen klinischen Anwendung zu

bestätigen. Anknüpfend sollte vorzugsweise untersucht werden, ob die erhöhten striatalen und kortikalen Fehlersignale zum einen auf ein hyperaktives Handlungsüberwachungs-System deuten und zum anderen mit abgeschwächter klinischer Effektivität in Verbindung gebracht werden können.

1. Introduction

1.1. Obsessive-compulsive disorder

Obsessive-compulsive disorder (OCD) is a psychiatric illness that is characterized by recurrent, stereotyped and intrusive thoughts (obsessions) and/or repetitive, ritualized behaviors (compulsions; (Murray & Lopez, 1996)). OCD is one of most common psychiatric disorders with a lifetime prevalence of 0.1-2.3% and around 2.9 million affected in the European Union (Wittchen, et al., 2011). Despite guideline based treatments, including cognitive-behavioral therapy and pharmacotherapy (Koran, et al., 2007), the response and remission rate is between 20 and 70% and OCD symptoms often persist at moderate levels (Eddy, Dutra, Bradley, & Westen, 2004; Grados & Riddle, 2008). For severely affected treatment resistant patients, an option of treatment with deep brain stimulation (DBS) is available, that will be introduced further in section 1.1.3.

1.1.1. Pathophysiology of obsessive-compulsive disorder

OCD has been associated with dysfunctional cortico-striato-thalamo-cortical circuits (CSTC (Beucke, et al., 2013; Harrison, et al., 2009; McIntyre & Hahn, 2010; Shephard, et al., 2021), that are implicated in higher order cognitive functions. At this point, close consideration is required to the affected frontostriatal circuit that is substantially involved in goal-directed behavior, including the basal ganglia motor circuit. (Shephard, et al., 2021; B. Zavala, Zaghloul, & Brown, 2015). Briefly, this CSTC circuit interconnects the mediofrontal cortex (MFC) via cognitive and limbic parts of the basal ganglia with the thalamus, which finally connects back to the cortex (Figure 1A; (Shephard, et al., 2021; B. Zavala, et al., 2015)). More specifically, information can be processed via three pathways within this circuit: the direct pathway, the indirect pathway, and the hyperdirect pathway. Via the direct (excitatory) pathway, the striatum gates motor selection based on information delivered by the cortex via direct inhibition of globus pallidus interna and the substantia nigra (GPi/SNr) resulting in thalamic disinhibition and thus inducing motor responses (Frank, 2006). Via the indirect (inhibitory) pathway, the striatum inhibits globus pallidus externa resulting in disinhibition of the nucleus subthalamicus (STN). Increased activation of the STN provides excitation of (GPi/SNr) and thus inhibition of the thalamus and thereby inhibition of the motor response. Finally, via the hyperdirect (inhibitory) pathway cortex directly activates the STN leading to fast thalamic inhibition.

During a simple selection of goal-directed behavior, frontostriatal activity related to the response reaches a certain decision-threshold and is conveyed by the direct pathway (parallel to the transmission of the alternative response by the indirect inhibitory pathway, preventing its execution).

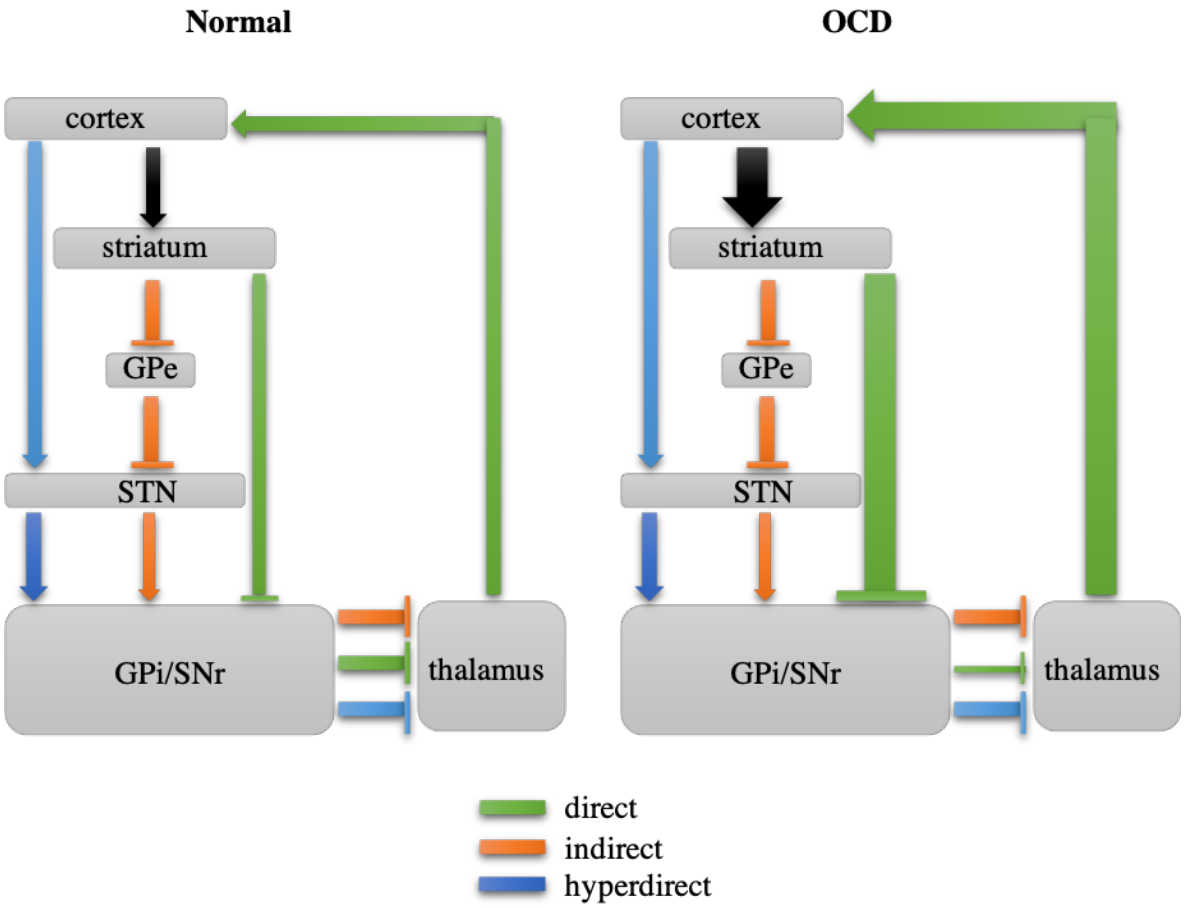

Figure 1 Simplified cortico-striato-thalamo-cortical circuit (CSTC). A) Cortical structures convey information to striatum, the main input structure of the basal ganglia. Through the direct pathway, striatal inhibition of the globus pallidus interna and the substantia nigra (GPi/SNr) leads to a disinhibition of the thalamus, which excites the cortex. Through the indirect pathway, the striatum inhibits globus pallidus externa (GPe) leading to a disinhibition of the nucleus subthalamicus (STN). The STN excites the GPi/SNr resulting in inhibition of the thalamus. Through the hyperdirect pathway, STN is directly excited by the cortex and activates the GPi/SNr, leading to inhibition of the thalamus. B) In OCD, a decreased excitatory threshold leads to an overactivation of the direct pathway. Figure modified after Pauls, Abramovitch, Rauch, and Geller (2014); Wiecki and Frank (2013)

In the case of ambiguous or incompatible stimuli presentation, two competing response tendencies are generated. MFC detects the presence of conflict and activates the hyperdirect pathway. This leads to a global inhibition of all corticostriatal inputs, and therefore to elevation of the cortical decision-threshold, so that stronger signals are needed to overcome the inhibition,

providing more time to resolve the conflict (Cavanagh, et al., 2011). Meanwhile, unlike the evidence for the prepotent response, the evidence for the alternative response steadily rises, eventually reaching the threshold and activating the excitatory pathway for response selection (Frank, 2006; Wiecki & Frank, 2013; B. Zavala, et al., 2015).

In OCD, a reduced activity of striatal interneurons causes a disbalance between pathways resulting in an overexpression of the direct excitatory pathway compared to the inhibitory pathways (Figure 1B; (Burguiere, Monteiro, Mallet, Feng, & Graybiel, 2015)). It is in particular associated with hyperactivity in the cortex and in the striatum and additionally with frontostriatal hyperconnectivity (Ahmari, et al., 2013; Beucke, et al., 2013; Winter, et al., 2019). These alterations interfere with several cognitive processes like goal-directed behavior and inhibitory control and result in overactive performance monitoring (Endrass & Ullsperger, 2014; Fitzgerald, et al., 2005; W. J. Gehring, Himle, & Nisenson, 2000; Gu, et al., 2008; Melcher, Falkai, & Gruber, 2008). Further account of the performance monitoring system and its alterations in OCD are given below. It remains to be emphasized, that MFC as well as the striatum and the frontostriatal network are implemented in the pathophysiology of OCD.

1.1.2. Deep brain stimulation

Deep brain stimulation (DBS) is a neuromodulative treatment involving neurosurgical, stereotactic implantation of electrodes into particular subcortical regions. The implanted impulse generator mostly provides chronic electrical high-frequency stimulation (~130 Hz) via the implanted electrodes in order to modify disease-related networks and restore functional brain activity. The DBS procedure has evolved from ablative surgery, e.g. thalamotomy (Benabid, Pollak, Louveau, Henry, & de Rougemont, 1987) and surpasses its value by showing less side effects, being adjustable and reversible while providing comparable clinical efficacy. Meanwhile, for about thirty years DBS is an established treatment option for movement disorders such as Parkinson's disease, dystonia and tremor (Krack, Volkmann, Tinkhauser, & Deuschl, 2019). This therapeutic success and clinical observations of psychiatric effects in patients with Parkinson's disease treated with DBS, combined with an increasing understanding of networks underlying psychiatric disorders, motivated the application of DBS for psychiatric disorders (Kuhn, et al., 2010; Nuttin, Cosyns, Demeulemeester, Gybels, & Meyerson, 1999). For about twenty years, DBS has been applied in psychiatric disorders such as OCD, depression, Tourette syndrome, substance abuse disorders and Alzheimer’s disease (Holtzheimer & Mayberg, 2011; Kuhn, et al., 2010).

1.1.3. Deep brain stimulation in obsessive-compulsive disorder

DBS therapy has been shown to be beneficial for treatment resistant patients with responder rates around 60% and over 35% symptom reduction as measured on the Yale-Brown Obsessive Compulsive scale (Y-BOCS; (Denys, et al., 2020; Goodman, et al., 1989; Huys, et al., 2019; Kohl, et al., 2014; van Westen, Rietveld, Figee, & Denys, 2015)). DBS in several brain regions induced comparable symptom improvements (Alonso, et al., 2015; Kohl, et al., 2014). Noteworthy, most of these targets lie within the frontostriatal circuit and involve similar connections (Haber, Yendiki, & Jbabdi, 2020). The focus of this dissertation will be on one particular striatal target, the anterior limb of internal capsule (ALIC) and nucleus accumbens (NAc), often referred to as "ALIC/NAc". DBS targeted in the ALIC/NAc has been approved by the U.S. Food and Drug Administration under the Human Device Exemption as a therapy option for treatment refractory OCD patients (Denys, et al., 2020; Denys, et al., 2010; Goodman, et al., 2010; Greenberg, et al., 2010; Huys, et al., 2019). Notably, white matter bundles of the ALIC comprise the hyperdirect pathway of the CSTC loop described above (Li, et al., 2020). Further account of ALIC/NAc is given in section 1.3.

Although, the mechanisms of DBS in OCD have not yet been sufficiently explored (Veerakumar & Berton, 2015) the modulatory effects beyond the target region, particularly involving frontostriatal networks including ALIC/NAc and MFC, are considered to play a key role (Figee, et al., 2013; Smith, Schuller, Huys, Baldermann, Andrade, et al., 2020; Smith, Schuller, Huys, Baldermann, Ullsperger, et al., 2020). Remarkably, DBS of the NAc in OCD reduced striatal and cortical hyperactivity as well as hyperconnectivity between these regions (Figee, et al., 2013). Moreover, decline of the hyperconnectivity correlated with symptom improvement. Notably, effective modulation of hyperdirect ALIC fibers connecting MFC and STN are related to clinical efficacy (Baldermann, et al., 2019; Li, et al., 2020). Accordingly, the general view is that effective DBS is dependent on targeting white-matter networks rather than discrete cortical or subcortical structures (Haber, et al., 2020). In sum, targeting the hyperdirect pathway of the described CSTC circuit with DBS recovers dysfunctions associated with this circuit. Hence, effects on goal-directed behavior and performance monitoring are conjecturable and will be considered in the following.

1.2. Performance monitoring

One crucial cognitive function, particularly in the context of goal-directed behavior, is the monitoring of ongoing performance. This involves the registration and evaluation of crucial information about current states, actions and their consequences. If necessary, the performance monitoring system initiates behavioral adjustments in order to optimize future behavior. Performance monitoring is primarily accomplished by brain structures interconnected in the frontostriatal CSTC circuit. For the investigation of performance monitoring functions, various cognitive tasks have been established, one of which is introduced below.

1.2.1. Flanker task

From a variety of different cognitive tasks, the Eriksen flanker task (Eriksen & Eriksen, 1974) has become well-established in performance monitoring research, particularly for investigation of conflict- and error-related effects on task performance and electroencephalographic signals (Danielmeier, Wessel, Steinhauser, & Ullsperger, 2009; Fischer, Klein, & Ullsperger, 2017; Kopp, Rist, & Mattler, 1996). During the computer-based arrow version of the task, arrows are presented on a screen, whereby only the middle arrow (target) is relevant for the participants response (Figure 2). The other, response-irrelevant arrows (flankers) are positioned above and below the target. They can have the same (congruent) or the opposite (incongruent) orientation as the target. The aim of the incongruent orientation is to distract the participant and to initiate task processing that increases the probability of erroneous motor execution. To increase this effect, the flankers are presented 80 ms earlier than the target. Furthermore, the participants have to respond quickly due to fast shift between trials.

The incongruent condition evokes larger decision conflict than congruent condition, because the processing of the irrelevant flankers interfere with the processing of the relevant target (Danielmeier, et al., 2009). Particularly, as described in the context of the CSTC loop (see section 1.1.1), in that case response pathways for both, correct and incorrect, responses are concurrently activated. The thereby detected conflict induce global inhibition, providing more time for the evidence accumulation for the correct response, in other words for conflict resolution. Accordingly, the reaction times of correct incompatible trials are larger than of correct compatible trials, where processing is not retarded by global inhibition.

Furthermore, as compared to compatible condition, the incorrect response pathway is particularly often activated in incompatible condition (possibly slightly earlier than the correct

pathway). In cases of insufficient inhibition and/or due to increased noise during processing the premature false response becomes selected resulting in performance errors. Thus, incompatible condition leads to higher amount of performance errors that the compatible condition. The reaction time of performance errors is thereby faster than during correct performance, where the response selection process is mature.

Remarkably, the differing conditions regarding decision conflict and erroneous responses in the flanker task were found to reliably elicit modulations in electroencephalographic correlates of performance monitoring (Danielmeier, et al., 2009; Fischer, et al., 2017; Trujillo & Allen, 2007; Yeung, Botvinick, & Cohen, 2004). In total, the flanker task is particularly suitable for the investigation of processes and electroencephalographic correlates related to decision conflict and error processing. An introduction in the electroencephalography (EEG) and correlates of performance monitoring is given below.

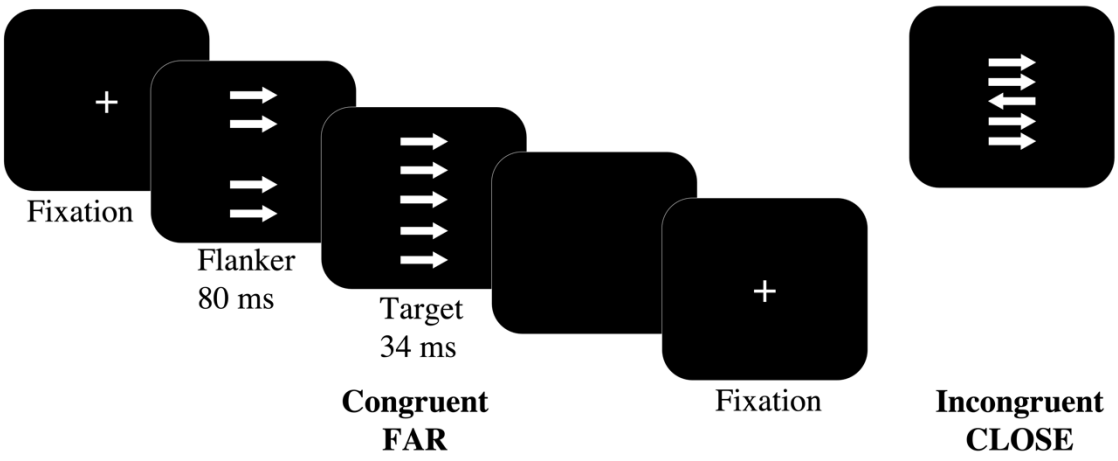

Figure 2 Experimental design of the custom version of the Erikson Flanker task. Patients have to respond accordingly to the target arrow orientation with a button press. The conditions varied regarding the congruency (congruent, incongruent) and distance (far, close) between the target arrow and the flankers. Modified from Sildatke, et al. (2020)

1.2.2. General introduction of electroencephalography

A powerful research method for performance monitoring is electroencephalography (EEG). EEG is a non-invasive method for assessing cortical activity through electrodes placed on scalp (Seifert, 2005). Part of the measured activity represents dipoles generated by postsynaptic potentials of multiple simultaneously active neurons during signal transmission.

Although its spatial resolution is limited compared to functional magnetic resonance imaging (fMRI), EEG has excellent temporal resolution in the order of milliseconds. The high temporal fidelity is particularly suitable for investigation of rapidly changing brain activity during cognitive processes.

Another, though less accessible possibility to measure electrophysiological brain activity is by means of local-filed potentials (LFPs). LFPs describe brain activity from subcortical structures, e.g., as recorded via implanted DBS macroelectrodes. Alike the EEG signal, LFPs reflect synchronous fluctuations caused by synaptic activity from large group of neurons (Buzsáki, Anastassiou, & Koch, 2012). Thereby, any transmembrane current is believed to contribute to extracellular voltage deflection that is captured by the LFPs. Particularly, the LFP comprises signals derived from within 0.5 to 3mm of the electrode contact (Munte, et al., 2008). Although neurons of subcortical structures primarily do not share the cortex's laminar architecture, that is well suited for generation of dipole signals, the neuronal organization still enables LFP generation, for example in the basal ganglia including striatum, though its extent might be reduced depending on the location (Brown & Williams, 2005). Accordingly, the amplitude and frequency of LFPs depend on relative input of multiple sources and on characteristics of the brain tissue (Buzsáki, et al., 2012).

In performance monitoring research, EEG investigations are often focused on signals that are evoked or triggered by task events (e.g., visual, auditory, haptic stimuli) and become evident after averaging multiple of trials, thus by improving the signal to noise ratio (Luck, 2005). There are various approaches for investigation of evoked EEG data, while in this dissertation I will focus on the following two.

1.2.2.1. Evoked EEG signal in time-frequency domain

The EEG signal can be viewed as a mixture of different sinusoidal oscillations (Cohen, 2014; Handy, 2005). A sine wave can be described by three characteristics: frequency, power and phase. Frequency describes the speed of the oscillation (cycles per second; Hz). Power (or amplitude) describes the amount of energy of a frequency band (dB). Phase describes the position along the signal over the time (radian or degree). To obtain information about the evolvement of oscillations of specific frequency-band over time one can use the wavelet transform. A wavelet is a short wave-like oscillation of definite frequency (Cohen, 2014; Handy, 2005). By convoluting the EEG signal with a wavelet, the signal is broken up and compared with versions of the wavelet over time yielding information about power and phase

of the oscillation for each time point. Thus, changes in power of predefined frequency-band induced by task events over a time period can be detected. Besides, phase information can be used for investigation of the degree of coupling between phases of different brain areas (phase-synchronization), indicative for long-distance communication (Vinck, Oostenveld, van Wingerden, Battaglia, & Pennartz, 2011).

The oscillatory activity usually consists of twofold signals, synchronized (phase-locked to the trigger) and not synchronized in phase (non-phase locked). The phase-locked activity of an oscillatory signal can also be evaluated in time domain analyses by means of event-related potentials (see section 1.2.2.2).

1.2.2.2. Evoked EEG signal in time domain: Event-related potentials

Another approach of EEG-investigation is the measure of event-related potentials (ERP). These are evoked deflections in the EEG signal measure that are phase-locked to the eliciting stimulus. ERPs are typically characterized by three specific parameters: amplitude peak (inclusive polarity), latency and topography (Luck, 2005; Seifert, 2005). Amplitude peak describes the amount of maximal deflection of the waveform (in μV) whereby its sign depends on the polarity of the waveform. Latency of a potential describes the time delay (ms) between the trigger and the peak. Topography describes the spatial distribution of the EEG signal over the scalp enabling to determine the position (electrode) with the maximum signal expression.

Several event-related frequency-specific modulations as well as ERPs were found to correlate with distinct processes of performance monitoring (Ullsperger, Danielmeier, & Jocham, 2014). Those included in this dissertation are introduced in section 1.2.3.

1.2.3. General introduction in the correlates of performance monitoring

1.2.3.1. Conflict-theta

While performing a cognitive (flanker) task, decision conflict emerges in the presence of competing response tendencies induced by ambiguous or incompatible stimuli. In this case, MFC signals the need for enhanced cognitive control to the STN via the hyperdirect pathway (Frank, 2006; B. Zavala, et al., 2013; B. A. Zavala, et al., 2014). This signal is mediated by increase of oscillatory activity in the theta frequency band (3-7 Hz; (Cavanagh, Cohen, & Allen, 2009; Cavanagh & Frank, 2014; Cavanagh, Zambrano-Vazquez, & Allen, 2012; Cohen & Cavanagh, 2011; Trujillo & Allen, 2007)).

At the cognitive level, theta is associated with conflict monitoring in this particular scenario but has further been linked to error monitoring (see next section) and feedback processing (Cohen, Elger, & Ranganath, 2007; Luu & Tucker, 2001). Theta frequency modulation is further involved in communication of the cortical areas with spatially distant regions. This has been confirmed by reveling theta synchronization between MFC and NAc (Cohen, et al., 2009c; Cohen, et al., 2012; Eijsker, van Wingen, Smolders, Smit, & Denys, 2020; Horschig, et al., 2015). In sum, theta frequency modulations provide a mechanism for MFC to coordinate local and long-range neural networks and is involved in performance monitoring and cognitive control.

Conflict-related theta power from the MFC, henceforth "MFC-conflict-theta", can be measured with EEG and is centered over mid-frontal electrodes (i.e., FCz: fronto-central electrode with zero cm distance from midline; (Cohen & Cavanagh, 2011; Cohen, Ridderinkhof, Haupt, Elger, & Fell, 2008)). According to the stated background, the MFC-conflict-theta increases with greater decision conflict.

1.2.3.2. Error-theta

As already mentioned, tasks containing high decision conflict particularly evoke performance errors, especially if speed is emphasized over accuracy. Analogous to the processing of decision conflict, monitoring of performance errors in the MFC is also mediated by oscillatory activity in the theta frequency band (Cavanagh, et al., 2009). Error-related theta additionally provides long-range communication between neuronal networks (Cohen, 2011).

The error-related theta power, henceforth "MFC-error-theta", is measurable with EEG and is greater after performance errors compared to correct responses (Figure 3; (Luu, Tucker, & Makeig, 2004; Trujillo & Allen, 2007)). It is considered to reflect the monitoring of performance errors and to subsequently provide signals for required cognitive control and behavioral adaptations to prevent future errors. Notably, modulations of MFC-error-theta are dependent on the strength of structural frontostriatal connectivity (Cohen, 2011).

The phase-locked activity of MFC-error-theta can also be revealed by ERP-analysis which is frequently utilized for investigation of monitoring of performance errors. The corresponding correlate is introduced in the following section.

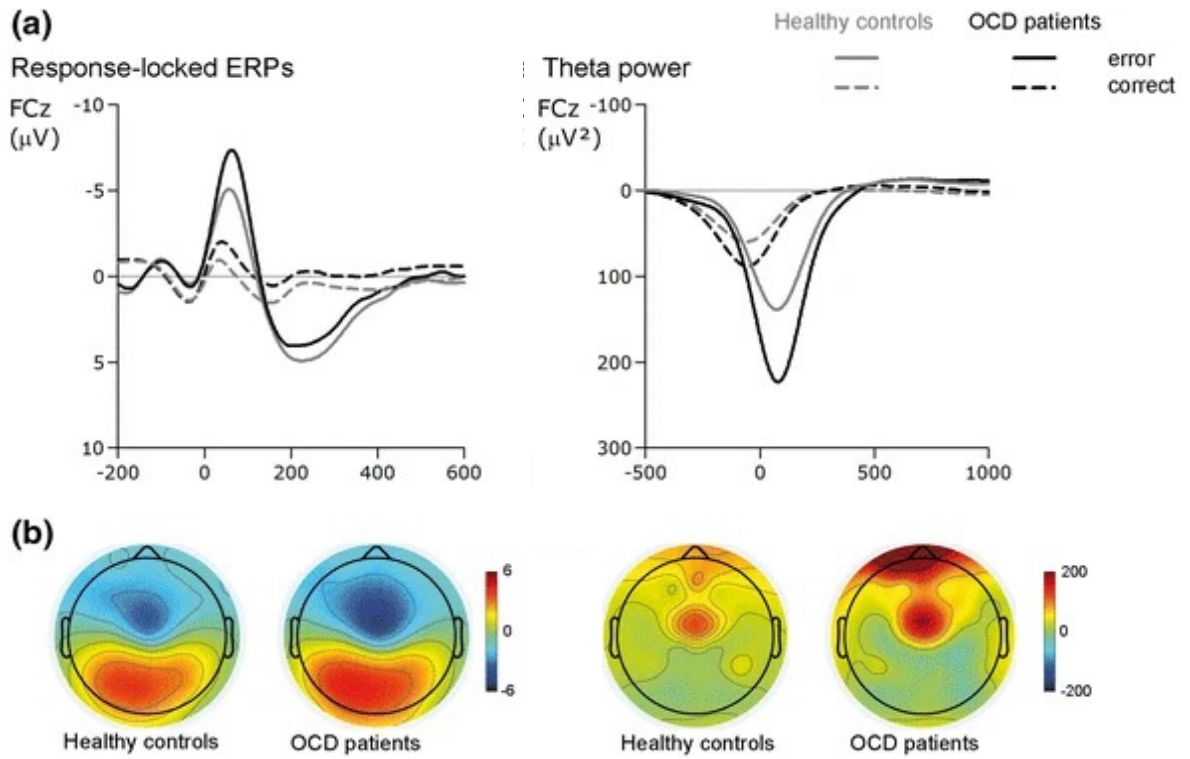

Figure 3 Error-related EEG-correlates. A) Grand average waveforms at electrode FCz for the ERPs (ERN and CRN, left) and theta power (right; 4–8 Hz) for healthy comparison participants (gray lines) and OCD patients (black lines) for errors (solid lines) and correct reactions (dashed lines). B) Topographies for ERN (left), and theta power (right) for healthy comparison participants and OCD patients. Note ERPs were filtered with a 15-Hz low-pass filter for visual presentation. Figure modified from (Riesel, Kathmann, & Endrass, 2014)

1.2.3.3. Error-related negativity (ERN)

Investigations of EEG-correlates of erroneous performance implemented especially frequent ERP-analysis. The corresponding potential is the well-studied error-related negativity (ERN), a negative deflection peaking at 50-150 ms after an incorrect task response (Danielmeier, et al., 2009; Falkenstein, Hohnsbein, Hoormann, & Blanke, 1990; Falkenstein, Hoormann, Christ, & Hohnsbein, 2000; William J. Gehring, Goss, Coles, Meyer, & Donchin, 2016; Riesel, 2019). The ERN is generated in the posterior MFC and is maximal at mid-frontal electrodes (i.e., FCz; Figure 3).

Despite many investigations of the ERN its underlying processes are not clearly identified. It is assumed that the ERN reflects error related processes, like error detection, signaling the requirement of cognitive control and leading to its adjustments in favor of error prevention (Botvinick, Braver, Barch, Carter, & Cohen, 2001; Falkenstein, Hohnsbein, Hoormann, & Blanke, 1991; William J. Gehring, et al., 2016; Holroyd & Coles, 2002; Ullsperger, Danielmeier, et al., 2014; Ullsperger, Fischer, Nigbur, & Endrass, 2014).

Studies often report an ERN-like but smaller deflection after correct responses, the so-called correct-related negativity (CRN; (Coles, Scheffers, & Holroyd, 2001; Falkenstein, et al., 2000)). Both, the ERN and CRN have similar timing and topography, but it is still unclear whether they reflect identical processes. Though, the CRN appears to arise by uncertainty about the response outcome and likely initiates behavioral adjustments to improve performance (Bartholow, et al., 2005; Ullsperger, Danielmeier, et al., 2014).

1.2.4. EEG-correlates in OCD

Several alterations of performance monitoring correlates have been reported in OCD (Endrass & Ullsperger, 2014; Perera, Bailey, Herring, & Fitzgerald, 2019). Correlates of decision conflict, i.e. amplitudes in time-resolved EEG signal, are increased in OCD compared to healthy controls, indicating enhanced or excessive recruitment of cognitive control during decision conflict (Riesel, Klawohn, Kathmann, & Endrass, 2017).

Further, EEG signals during error processing are larger in OCD than healthy controls ((Endrass & Ullsperger, 2014; Perera, et al., 2019); Figure 3)). Specifically, MFC-error-theta was enhanced in OCD after both, error and correct responses (Riesel, et al., 2014). Moreover, the ERN amplitude was consistently increased, representing the most replicated finding in EEG research with OCD patients (Carrasco, et al., 2013; Endrass, Klawohn, Schuster, & Kathmann, 2008; Endrass, et al., 2010; Grundler, Cavanagh, Figueroa, Frank, & Allen, 2009), but see Kaczkurkin (2013) for absent ERN alterations in OCD during a difficult task. These results support the notion of overexcited error processing in patients with OCD.

Generally, enhanced ERN in OCD seems to be independent from symptom severity and does not correlate with symptom scores (Endrass, et al., 2010; Riesel, Endrass, Kaufmann, & Kathmann, 2011; Riesel, et al., 2014), but see (Endrass, et al., 2008; W. J. Gehring, et al., 2000) for converse findings. In accordance, ERN enhancement persisted after symptom reduction (Hajcak, Franklin, Foa, & Simons, 2008; Riesel, Endrass, Auerbach, & Kathmann, 2015). Thus, the enhanced ERN in OCD seems to be independent of clinical symptoms and might represent the biological vulnerability to OCD. Accordingly, altered ERN has been suggested to be a candidate endophenotype for OCD (Hajcak, et al., 2008; Riesel, 2019; Riesel, et al., 2011) and to function as biomarker that may place individuals at risk for developing OCD (Endrass & Ullsperger, 2014; Riesel, et al., 2014).

Noteworthy, mostly no differences were observed in task performance between OCD patients and healthy participants, i.e. regarding accuracy and reaction times. The preservation of normal-range performance with concurrent elevation of activity measured with EEG indicate that stronger signals are required for a sufficient control during decision conflict and error processing in OCD. This is in with the view of overactive performance monitoring system in this disorder.

1.3. DBS target structure ALIC/NAc and its role in performance monitoring

The NAc is regarded as the core structure of the ventral striatum. It is considered a limbic-motor interface (Mogenson, Jones, & Yim, 1980) by integrating contextual information from hippocampus, emotional information from amygdala, and cognitive information from the cortex, and is therefore a crucial structure for goal-directed behavior (Goto & Grace, 2005; Grace, Floresco, Goto, & Lodge, 2007). NAc is an important part of this performance monitoring system what is reinforced by structural and functional connections between NAc and further essential regions of performance monitoring system, including the MFC (Brady & O'Donnell, 2004; Haber, Fudge, & McFarland, 2000; Haber & Knutson, 2010; Haber, Kunishio, Mizobuchi, & Lyndbalta, 1995; Jackson, Frost, & Moghaddam, 2001; Salgado & Kaplitt, 2015; Ullsperger, Danielmeier, et al., 2014). Thus, it would suggest itself that activity in the NAc is related to electrophysiological activity during performance monitoring. Indeed, some studies reported on an association of NAc functioning with the ERN. In detail, striatal lesions abolished the ERN (Ullsperger & von Cramon, 2006), whereas DBS stimulation in the NAc enhanced disease-related reduced ERN in patients with severe alcohol abuse disorder (Kuhn, et al., 2011). The opportunity of LFP-recording from the striatum through DBS electrode has moreover strengthened the link between cortical and striatal activity during error processing. Specifically, an ERN-like LFP was found in the NAc following performance errors in one patient with OCD (Munte, et al., 2007), in total in four patients with severe alcohol abuse disorder (Heinze, et al., 2009; Voges, Muller, Bogerts, Munte, & Heinze, 2013), and in four patients with severe opioid use disorder (Sildatke, et al., 2020). Additionally, enhancement of theta frequency power in the NAc was associated with performance errors (Eijsker, et al., 2020). Generally speaking, striatal LFP activity seems to be modulated during processes requiring increased cognitive demand and behavioral adaptation (Cohen, et al., 2009a, 2009b; Widge, et al., 2019). Further interrelation between MFC and NAc is supported by several studies reporting a performance-related functional connectivity as revealed by coherence and/or phase

synchronization at theta frequency, for example, prior to behavioral adaptations (Cohen, et al., 2009c), behavioral inhibition (Eijsker, et al., 2020), and performance feedback (Schuller, et al., 2015).

The ALIC is a white matter structure entailing numerous fibers that primarily interconnect cortical structures with STN and thalamus, all structures that are involved in cognitive circuits and compose the hyperdirect pathway (Baldermann, et al., 2019; Mithani, Davison, Meng, & Lipsman, 2020). Many ALIC fibers are also embedded within the striatum and are regarded as part of the ventral striatum rather than the ALIC (Haber, et al., 2020; Mithani, et al., 2020). Particularly applying stimulation in ALIC has been related to clinical efficacy in OCD (Baldermann, et al., 2019; Li, et al., 2020). Remarkably, the frontostriatal hyperconnectivity in OCD patients was reduced by effective striatal stimulation potentially via decreasing theta synchronization between these regions (Figee, et al., 2013; Smolders, et al., 2013). Additionally, DBS-induced changes also concerned modulations of striatal activity during performance monitoring, e.g., conflict-related theta (Widge, et al., 2019). Taken together, there are several indications for a crucial role of the DBS target region ALIC/NAc in decision conflict and error-related performance.

1.4. Objectives

ALIC/NAc has become an important target for DBS treatment in OCD. A profound understanding of its the functional role in performance monitoring is not only an exciting aspect of fundamental research but might furthermore advance the sparse knowledge about the mode of action of DBS and further our understanding of brain networks crucial for OCD. Despite of steadily growing evidence our knowledge is still limited regarding the involvement of ALIC/NAc in conflict monitoring, error processing and the associated electrophysiological correlates. This is mainly due to the fact that intracranial EEG recordings in human are rare to obtain. The first aim of this dissertation is to extend this knowledge within the scope of the **LFP-study** and investigate conflict- and error-related activity in the ALIC/NAc, whereby detailed hypotheses are outlined below.

In addition, despite of common application of the ALIC/NAc as a target for DBS in OCD, the knowledge regarding the stimulation effects on performance monitoring is still sparse. Expanding these insights might facilitate to discover the mode of action for DBS regarding clinical efficacy in OCD. Accordingly, the second aim of this dissertation is to

investigate the DBS effects on EEG-correlates of conflict monitoring and error processing in our **Stimulation-study**, which detailed hypotheses are outlined below.

1.4.1. LFP-study

The first aim of this dissertation is to explore whether ALIC/NAc is particularly involved in conflict- and error-related processes that are known to be altered in OCD. To this aim, we synchronously recorded EEG and ALIC/NAc LFPs in patients with OCD performing a flanker task. Based on the stated background we assumed that correlates of conflict monitoring (conflict-theta), and error processing (error-theta and ERN) are not only expressed in the MFC but can also be found in the ALIC/NAc. Accordingly, we formulated the following hypotheses:

1.1. We expected larger EEG modulations at electrode FCz in the theta frequency (MFC-conflict-theta) during high-conflict trials (i.e. incongruent flankers) than during low-conflict trials (i.e. congruent flankers), reflecting larger cognitive control demands to resolve decision conflict.

1.2. We expected larger ALIC/NAc LFP modulations in the theta frequency (LFP-conflict-theta) during high-conflict trials (i.e. incongruent flankers) than during low-conflict trials (i.e. congruent flankers), reflecting larger cognitive control demands to resolve decision conflict.

1.3. Following response errors, we expected theta frequency power at electrode FCz to be increased for response errors compared to correct responses, reflecting larger cognitive control demands during the processing of errors.

1.4. Following response errors, we expected theta frequency power of ALIC/NAc LFPs to be increased for response errors compared to correct responses, reflecting larger cognitive control demands during the processing of errors.

1.5. Following response errors, we expected the ERP at electrode FCz to be increased for response errors compared to correct responses, reflecting larger cognitive control demands during the processing of errors.

1.6. Following response errors, we expected the ERP of ALIC/NAc LFPs to be increased for response errors (LFP-ERN) compared to correct responses, reflecting larger cognitive control demands during the processing of errors.

Further, we expected to observe functional frontostriatal connectivity in the theta-frequency band during conflict monitoring and error processing. We hypothesized that

1.7. Functional frontostriatal connectivity in the theta frequency band is modulated by decision conflict (low vs. high). In particular, we expected larger connectivity during high- compared to low-conflict, reflecting increased network communication to enhance cognitive control for conflict resolution.
1.8. Functional frontostriatal connectivity in the theta frequency band is modulated by error processing (correct vs. error). In particular, we expected increased connectivity during processing of error compared to correct responses, reflecting increased network communication to enhance cognitive control during processing of errors.

Finally, because of specified associations on DBS-induced symptom reductions with changes of striatal activity (e.g. Figee, et al., 2013), we wanted to explore possible interrelation of the OCD-symptom score and observed LFPs and frontostriatal connectivity. In detail, we wanted to explore whether

1.9. LFP-conflict-theta in the ALIC/NAc correlates with pre-surgery symptom severity.
1.10. LFP-error-theta in the ALIC/NAc correlates with pre-surgery symptom severity.
1.11. LFP-ERN in the ALIC/NAc correlates with pre-surgery symptom severity.
1.12. Functional frontostriatal connectivity during conflict monitoring correlates with pre-surgery symptom severity.
1.13. Functional frontostriatal connectivity during error processing correlates with pre-surgery symptom severity.
1.14. LFP-conflict-theta in the ALIC/NAc correlates with symptom improvement after DBS.
1.15. LFP-error-theta in the ALIC/NAc correlates with symptom improvement after DBS.
1.16. LFP-ERN in the ALIC/NAc correlates with symptom improvement after DBS.
1.17. Functional frontostriatal connectivity during conflict monitoring correlate with symptom improvement after DBS.
1.18. Functional frontostriatal connectivity during error processing correlate with symptom improvement after DBS.

1.4.2. Stimulation-study

Evaluating the effects of ALIC/NAc stimulation on performance monitoring EEG-correlates can provide important insights in the therapeutic mode of action of DBS treatment. Thus, the second aim of this dissertation is to evaluate the effects of ALIC/NAc DBS on cortical correlates of conflict monitoring (i.e. MFC-conflict-theta) and error processing (i.e. ERN). To this aim, we compared MFC-conflict-theta/ERN of OCD patients before DBS implantation and with clinically effective stimulation settings in DBS-on and DBS-off states. We hypothesized that

2.1. The conflict monitoring during decision conflict is modulated by acute stimulation, which is indicated by decreased MFC-conflict-theta in DBS-on compared DBS-pre, reflecting downregulation of overactive conflict monitoring during active stimulation

2.2. The conflict monitoring during decision conflict is modulated by acute stimulation, which is indicated by decreased MFC-conflict-theta in DBS-on compared to DBS-off, reflecting upregulation of conflict monitoring after stimulation cessation.

2.3. The error processing is modulated by acute stimulation, which is indicated by decreased ERN amplitude in DBS-on compared to the DBS-pre, reflecting downregulation of overactive error processing during active stimulation.

2.4. The error processing is modulated by acute stimulation, which is indicated by decreased ERN amplitude in DBS-on compared to DBS-off, reflecting upregulation of error processing after stimulation cessation.

Furthermore, we wanted to explore possible interrelations linking the MFC-conflict-theta and the ERN to clinical efficacy of DBS, particularly whether

2.5. Symptom improvement after DBS correlates with pre-surgery MFC-conflict-theta

2.6. Symptom improvement after DBS correlates with pre-surgery ERN

2.7. Symptom improvement after DBS correlates with MFC-conflict-theta change induced by DBS (contrasting DBS-on and DBS-off)

2.8. Symptom improvement after DBS correlates with ERN change induced by DBS (contrasting DBS-on and DBS-off)

2. Methods

2.1. Participants

18 OCD patients participated in the aforementioned studies (7 male, mean age 43.4±13.5 years), whereby eleven patients participated in both studies while seven patients participated in either **LFP-study** or **Stimulation-study** (Table 1). Patients were otherwise treatment-refractory and received bilateral implantation of depth electrodes in the ALIC-NAc region for subsequent treatment with deep brain stimulation (DBS) as part of a clinical trial (see also Huys, et al. (2019); German Clinical Trial Register (www.drks. de, DRKS00005316)). Patients' demographical and clinical data is listed in Table 1. All patients were medicated at the time of the studies (Table 1). The ethics committee of the University of Cologne approved all procedures reported here as part of the clinical trial and all participants provided oral and written informed consent. The study was performed in accordance with the Declaration of Helsinki.

2.2. Task

In all studies, the participants performed a customized version of the Eriksen flanker task ((Danielmeier, et al., 2009; Eriksen & Eriksen, 1974); Figure 2). Stimuli were presented using Presentation (v10.3, Neurobehavioral Systems Inc., Albany, U.S.A.). During the task, participants had to respond to the orientation of the target arrow by pressing either the left or the right button, respectively. They were told to react as quickly and accurately as possible. On each trial four distractor stimuli (flankers) appeared at first and were followed 80 ms later by presentation of the target. The orientation of the flankers relative to the target was either the same (congruent) or the opposite (incongruent). In the employed customized version of the flanker task the distance between target and flankers additionally varied between close and far (Figure 2). This application enables further modulation of the degree of decision conflict, whereby close distance is linked to higher decision conflict compared to far distance (Danielmeier, et al., 2009). The distance between target and flankers in the close condition was 3.5° and 1.75° of visual angle below and above the center; in the far condition it was 6.5° and 4°. A colored frame instructed the participant during the task whether to speed up, to slow down or to maintain current speed level. This served to ensure a comparable accuracy-speed tradeoff across trials and participants. The response-stimulus interval varied from 750 to 1250 ms. The task contained four equally distributed conditions: 1) far compatible, 2) far incompatible, 3) close compatible, 4) close incompatible. In total, the task contained 800 trials which were

Table 1 Patients demographical and clinical information. Positive Y-BOCS change values indicate a symptom reduction; negative values indicate a symptom increase. *Ages have been rounded to the nearest decade to cover identities.

ID	Gender	Age*	Peri EEG	Pre/ postoperative EEG	Follow-up visit (months)	BDI pre	Y-BOCS pre	Y-BOCS% change (end of study)	Medication
1	m	60	Y	Y	6	18	32	75	-
2	f	30	Y	Y	12	12	33	33	Cl 50mg, A 50mg
3	m	60	Y	Y	6	4	25	28	Ch 160mg
4	m	30	Y	Y	6	19	26	38	M 10mg
5	m	60	Y	Y	6	29	36	39	F 100mg, Q 275mg, D 15mg, Z 7,5mg, Qm 900mg
6	f	40	Y	N	n.a.	19	30	73	Fl 80mg, Q 800mg, P 50mg, L 1mg
7	f	30	Y	Y	6	32	34	0	P 25mg
8	f	40	Y	Y	6	2	33	27	V 300mg
9	f	30	Y	N	n.a.	24	32	48	V 225mg, O 400mg, L 1mg
10	m	30	Y	N	n.a.	16	35	34	C 20mg,
11	f	50	Y	Y	6	15	32	31	Pa 40mg, Mi 15mg, Ap 5mg, P 50mg
12	f	30	Y	Y	6	22	37	8	Cl 150mg
13	f	50	Y	Y	6	33	34	65	V 75mg, Cl 100mg, Ol 20mg, P 50mg
14	m	50	Y	Y	12	14	28	54	L 1 mg, Cl 225mg, Q 300mg
15	f	30	N	Y	12	46	18	-22	E 30mg, Q 200mg, T 25mg
16	f	60	N	Y	6	20	25	20	Cl 150mg, P 100mg, Q 200mg
17	m	60	N	Y	6	41	26	-12	Pa 20mg, T 15mg
18	f	60	N	Y	12	35	35	29	Do 50mg, Fl 50mg
Total	7m/11w	43 ± 14	14/18	15/18	8 ± 3	22 ± 12	31 ± 5	32 ± 27	
LFP-study	6m/ 8w	41 ± 13	14/18	n.a.	n.a.	19 ± 9	32 ± 4	40 ± 22	
Stim.-study	6m/ 9w	46 ± 13	n.a.	15/18	8 ± 3	23 ± 13	30 ± 5	28 ± 27	

BDI: Beck Depression Inventory. A= Agomelatine, Ap=Aripiprazole, C= Citalopram, Ch= Chlorprothixen, Cl= Clomipramine, D= Diazepam, Do= Doxepine, E= Escitalopram, F= Fluvoxamine, Fl= Fluoxetine, L= Lorazepam, M= Memenatine, Mi=Mirtazepine, O= Opipramol, Ol= Olanzapine, P= Promethazine, Pa= Paroxetine, Q= Quetiapine, Qm= Quilonium, T= Trimipramine, V= Venlafaxine, Z= Zopiclon.

presented in a pseudo-randomized order in blocks of 100 trials. Performance feedback was given to the participants following each block including the number of correct responses. The task duration was about 25 minutes.

Trials with reaction times (RT) shorter than 150 ms or exceeding 1000 ms and trials containing response correction within 150 ms after the first response were excluded from analysis. This was done to remove trials containing unintentional or arbitrary responses and corrections whose activity might confound the investigating processes. Generally, the flanker task is particularly suitable for the investigation of EEG-correlates related to decision conflict and error processing, even in case of small number of trials (Fischer, et al., 2017). Nevertheless, to increase signal-to noise ratio we collapsed across close and far flanker conditions (Fischer, et al., 2017).

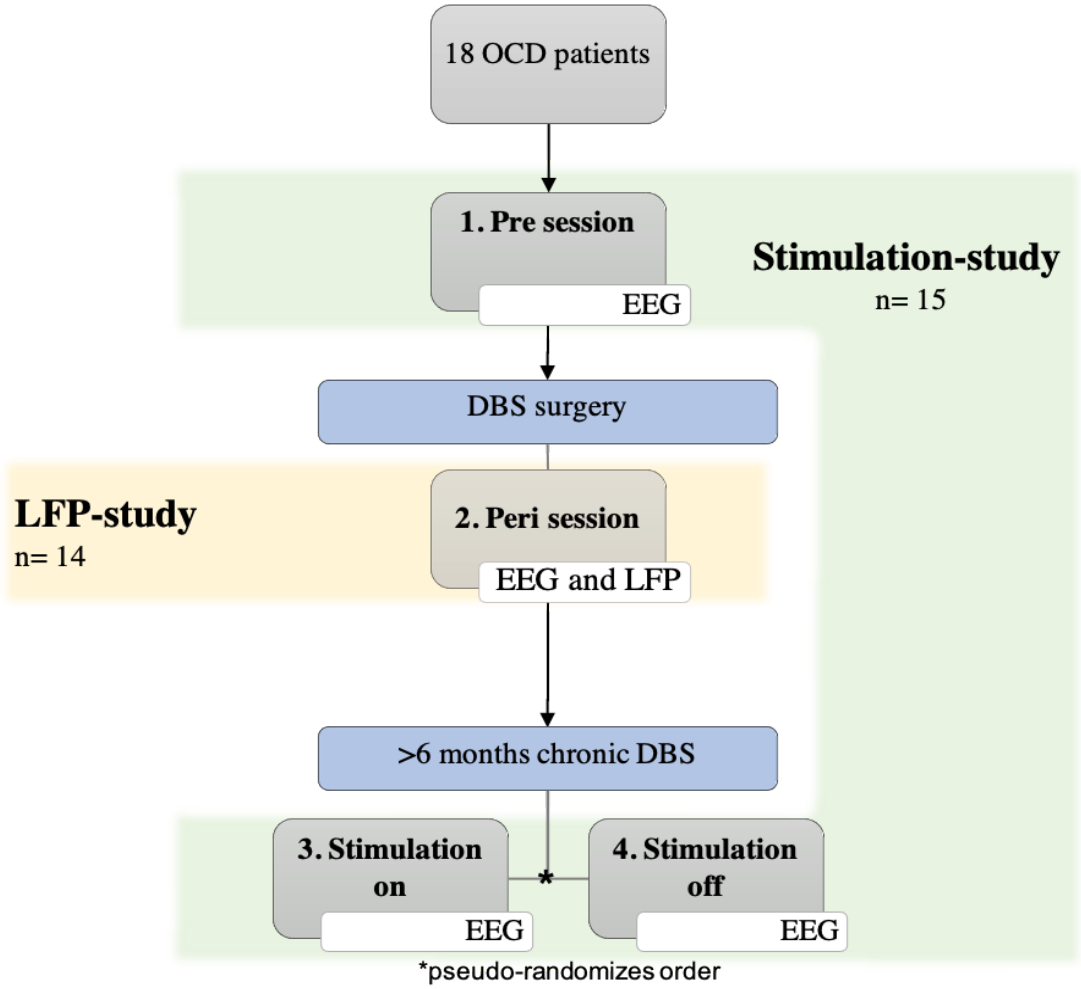

Figure 4 Design of the study. In total, patients' data were acquired at four recording sessions. For the **LFP-study**, one session was performed 24-48h after DBS surgery (peri). For the **Stimulation-study**, three sessions were performed: one before DBS surgery (pre) and two during follow-up visit, at least 6 months after DBS surgery with active stimulation (on) and with discontinued stimulation between 12 - 24 hours (off), respectively. The order of the on and off measurements was assigned pseudo randomly.

2.3. LFP-study

2.3.1. LFP-study: Data collection

Patients' data were acquired at one recording session 24-48h after DBS surgery (peri; Figure 4). Of the 18 subjects, four did not attend the peri session because of surgery related fatigue or due to organizational reasons, such as conflicting schedules or personnel absence (Table 1).

All recordings took place in a dimly lit, electronically, and acoustically shielded room. Because this session took place shortly after the surgery for DBS electrode implantation, patients had surgical incisions so that no EEG cap could be used for recordings of electrophysiological scalp data. Instead, scalp data were recorded using Au-electrodes (between 15 and 24, mean 20±3) that were placed individually by hand according to the extended 10-20 system (Jasper, 1958) and fastened with adhesive non-woven fabric. Because of surgical incisions the electrode placement varied but electrode FCz was always included. Further, LFPs were recorded from externalized depth electrodes targeted in the ALIC/NAc. These were quadripolar macroelectrodes (Medtronic 3387 or 3389; Medtronic, Inc., Minneapolis, MN, USA) with a lead contact width of 1.5 mm, diameter of 1.27 mm and 1.5 mm (model 3387) or 0.5 mm (model 3389) distance between contacts. The sampling rate during data recording was 5000 Hz (BrainAmp MR plus amplifiers; Brain Products, Gilching, Germany) and the impendences were kept below 15 kΩ.

Patients' symptom severity was assessed before DBS surgery and at the end of the clinical study (at least 12 months after surgery) using the Yale-Brown Obsessive Compulsive scale (Y-BOCS; (Goodman, et al., 1989)).

2.3.2. LFP-study: Data analysis

Data were processed using EEGLAB 14.1.1 (Delorme & Makeig, 2004) and custom Matlab 2017a routines (The Math Works Inc., Natick, U.S.A.). All data were filtered with cut-off frequencies of 0.5 and 40Hz (6dB/Octave) using a phase free finite impulse response filter and resampled to 500 Hz. LFPs were obtained from implanted depth electrode as follows. Each electrode contained four contacts: in the left hemisphere numbered as 0, 1, 2, 3 and in the right hemisphere numbered as 8, 9 ,10,11. The electrodes were implanted with the lower contact numbers located most ventral in the NAc and the higher contact numbers located most dorsal in the ALIC. LFPs were obtained by re-referencing two adjacent depth electrode contacts, resulting in maximally three bipolar channels per electrode. This method minimizes volume

conductance and captures locally generated activity (Marmor, et al., 2017). For further LFP analysis we selected middle or dorsal contacts depending on availability (13x 1-2 and 1x 2-3; 13x 9-10 and 1x 10-11).

Stimulus-locked epochs were extracted from -1500 ms to 2500 ms. Epochs that contained signals exceeding 5 standard deviations of the joint data probability were considered as outliers and were discarded to improve data quality. Eye movements and pulse artifacts were removed using Independent Component Analysis (ICA; (Makeig, Debener, Onton, & Delorme, 2004)). This method decomposes the data in independent components (ICs) with the aim to identify independent sources of variance in the signal. The selection of the respective ICs for removal occurred manually (rejected ICs peri: 1.2±1). Scalp data were re-referenced to linked mastoids because brain activity recorded here was expected to be smallest and also in order to avoid bias towards one hemisphere (Luck, 2005; Seifert, 2005).

All conflict-related analysis was performed on the stimulus-locked data in order to align the EEG activity on the stimulus presentation. Conflict-related theta- (conflict-theta) analysis was performed with incompatible and compatible correct trials, with the aim to observe merely the conflict effect and avoid influence from error-related processing.

Time-frequency decomposition was performed by convoluting data from single trials with Morlet wavelets: $e^{i2\pi tf}e^{-t^2/(2*\sigma^2)}$ where t is time, f is frequency, and σ specifies the width of each frequency band. f was set from 1 to 40 Hz and increased in 50 logarithmically spaced steps. σ was defined as $3.5/(2\pi f)$, where 3.5 specifies the number of wavelet cycles. Fast Fourier transform (FFT) was performed on the data and subsequently multiplied with the power spectrum of Morlet wavelets providing the power spectrum of the EEG data. Inverse FFT was applied resulting in complex signal. Out of this, frequency-specific power was defined as the value $Z(t) = \text{real}[z(t)]^2 + \text{imag}[z(t)]^2$). Power was normalized and baseline corrected using a decibel (dB) transform (dB power(tf) = 10*log10[power(tf)/baseline]). The baseline power for conflict-theta-analysis was set from -300 to -100 ms before stimulus.

Mean conflict-theta power was calculated from 3 to 7 Hz in the LFPs and at electrode FCz. The time window was centered ±100 ms around the grand average peak (averaged over high- and low-conflict trials and all electrodes of interest (FCz, left and right LFP) that was determined in a search window from 200 ms to 600 ms). The conflict-effect (Δconflict-theta) was calculated by subtracting the mean of the compatible trials from the mean of the incompatible trials. In the following, conflict-theta from electrode FCz is referred to as MFC-conflict-theta (effect as ΔMFC-conflict-theta), while conflict-theta from LFPs is referred to as LFP-conflict-theta (effect as ΔLFP-conflict-theta).

Functional frontostriatal connectivity at the time of conflict-theta was assessed by measuring phase-synchronization using debiased weighted Phase-Lag Index (dwPLI; (Vinck, et al., 2011)). dwPLI is a robust measure that is insensitive to volume conduction, sample size bias and gives reliable estimates despite moderate signal to noise ratios. For the analysis, bipolar DBS channels and bipolar rereferenced cortical channel FCz-Fz were used. Decomposition of time-frequency data was performed as described above. From results of the inverse FFT frequency-specific phase angle was obtained and the cross-spectrum density for the scalp-LFP electrodes was calculated. Its imaginary part I(x) was used for calculation of the connectivity coefficients dwPLI: $dwPLI=(E(I(x))^2 - E(I(x)^2)) / (E(|I(x)|)^2 - E(I(x)^2))$. The right sides of the numerator and denominator relate to debiasing coefficients. Values derived from the wPLI range between 0 and 1, whereby 0 indicates a random phase lag relationship across trials and 1 indicate a definite phase lag between both signals in all trials. Because of the debiasing coefficients, the values of the dwPLI can become negative which also indicate random relationship between signals. The averaged connectivity coefficients were calculated in theta frequency band (3 to 7 Hz) for compatible and incompatible condition. The change of the connectivity during conflict, the Δconflict-theta-connectivity, was calculated by subtracting the coefficients of compatible condition from the incompatible condition.

All error- or accuracy-related analyses were performed on response-locked data in order to align the EEG activity on the response execution. Therefore, data were extracted from -1300 ms to 1500 ms relative to the response. The number of error trials in the low-conflict (compatible) condition was quite small in most of the patients (mean 22±9 trials) and thus insufficient for an adequate signal-to-noise ratio needed for a reliable EEG-analysis (Fischer, et al., 2017). Thus, only high conflict (incompatible) error and correct trials were included in the analysis.

Error-related theta- (error-theta) analysis was performed corresponding to conflict-theta analysis. Particularly, time-frequency decomposition was performed by convoluting data from single trials with Morlet wavelets: $e^{i2\pi tf}e^{-t^2/(2*\sigma^2)}$ where t is time, f is frequency, and σ specifies the width of each frequency band. f was set from 1 to 40 Hz and increased in 50 logarithmically spaced steps. σ was defined as $3.5/(2\pi f)$, where 3.5 specifies the number of wavelet cycles. Fast Fourier transform (FFT) was performed on the data and subsequently multiplied with the power spectrum of Morlet wavelets providing the power spectrum of the EEG data. Inverse FFT was applied resulting in complex signal. Out of this, frequency-specific power was defined as the value $Z(t) = real[z(t)]^2 + imag[z(t)]^2$. Power was normalized and baseline corrected using a decibel (dB) transform (dB power(tf) =

10*log10[power(*tf*)/baseline]). The baseline power for error-theta-analysis was set from -300 to -100 ms before the response.

Mean error-theta power was calculated from 3 to 7 Hz in the LFPs and at electrode FCz. The time window was centered ±100 ms around the grand average peak (averaged over error and correct trials and all electrodes of interest (FCz, left and right LFP) that was determined in a search window from 0 ms to 200 ms). The error-effect (Δerror-theta) was calculated by subtracting the error-theta of correct trials from the error-theta of error trials. In the following, error-theta from electrode FCz is referred to as MFC-error-theta (effect as ΔMFC-error-theta), while error-theta from LFPs is referred to as LFP-error-theta (effect as ΔLFP-error-theta).

Functional frontostriatal connectivity at the time of error-theta was assessed by measuring phase-synchronization using dwPLI (Vinck, et al., 2011). For the analysis, bipolar DBS channels and bipolar rereferenced cortical channel FCz-Fz were used. Decomposition of time-frequency data was performed as described above. From results of the inverse FFT frequency-specific phase angle was obtained and the cross-spectrum density for the scalp-LFP electrodes was calculated. Its imaginary part I(x) was used for calculation of the connectivity coefficients dwPLI: $dwPLI=(E(I(x))^2 - E(I(x)^2)) / (E(| I(x) |)^2 - E(I(x)^2))$. The right sides of the numerator and denominator relate to debiasing coefficients. Values derived from the wPLI range between 0 and 1, whereby 0 indicates a random phase lag relationship across trials and 1 indicate a definite phase lag between both signals in all trials. Because of the debiasing coefficients, the values of the dwPLI can become negative which also indicate random relationship between signals. The averaged connectivity coefficients were calculated in theta frequency band (3 to 7 Hz) for incompatible error and correct condition. The change of the connectivity during error, the Δerror-theta-connectivity, was calculated by subtracting the coefficients of correct condition from the error condition.

Additionally, an ERP-analysis on error-related data was performed. Therefore, baseline correction was applied from -300 ms to -100 ms relative to stimulus onset and trials of each condition were averaged within subjects. The ERN/CRN amplitude was measured at electrode FCz and in the LFPs in error/correct trials.

By calculation of ERPs from bipolar LFPs, the polarity depends on the position of the two electrode contacts relative to the signal source and therefore minor shifts in electrode placement can lead to a polarity reversal. Thus, polarity is considered arbitrary in LFPs. Because we focused on error-related effects, we defined polarity on the course of the correct waveform, as described by Siegert, et al. (2014): the waveforms were realigned so that the first main deflection of the correct-related waveform was positive-going (resulting in the

realignment of 22 of 28 signals). We refer to polarity as 'negative' and 'positive' by this convention hereafter.

The ERN/CRN amplitudes at FCz were defined as mean amplitude ±40 ms centered around the subjects' grand average peak (search window 0 ms to 150 ms). The LFP amplitudes were calculated using the same time windows as for the ERN/CRN. We used this approach of amplitude measure instead of the more common approach of trough-to-peak amplitude measure for ERN/CRN (Falkenstein, et al., 2000; Kopp, et al., 1996) because no equivalent error/correct signal was characterized in the NAc so far. This way aimed to achieve consistency and to enhance comparative analysis of EEG and LFP data. For improved readability, these LFPs are referred to as LFP-ERN and LFP-CRN hereafter. The ERP-error-effect (ΔERN) was calculated by subtracting the CRN from the ERN.

2.3.3. LFP-study: Statistical analysis

Analysis of error rate of high-/low- conflict trials (compatible vs. incompatible) was performed using paired *t*-test. Analysis of RTs (correct compatible vs. incompatible; incompatible correct vs. error) was performed using paired *t*-test.

Condition differences (correct compatible vs. incompatible; incompatible correct vs. error) of scalp-recorded data were analyzed using paired *t*-test. To regard both hemispheres, LFP data were analyzed with repeated-measures analyses of variance (2 x 2 rmANOVA). Precisely, LFP-conflict-theta and coefficients of frontostriatal conflict-theta connectivity were analyzed with hemisphere (right, left) and compatibility (compatible, incompatible) as within-subject factors. LFP-error-theta, LFP-ERN and coefficients of error-theta connectivity were analyzed with hemisphere (right, left) and accuracy (correct, error) as within-subject factors. In additional exploratory analyses the coefficients of frontostriatal connectivity (conflict-theta and error-theta) were analyzed regarding their deviation from baseline using *t*-test.

Spearman correlation was performed to test the relationship between the symptom severity before DBS (Y-BOCS$_{pre}$) as well as their reduction at the end of the clinical study (in %; Y-BOCS$_{\%change}$) with LFP correlates. Particularly, LFP-conflict-effect (ΔLFP-conflict-theta), LFP-error-effect (ΔLFP-error-theta and ΔLFP-ERN) and the respective change in connectivity coefficients (ΔConnect conflict-theta and ΔConnect error-theta) were used for correlation. To counterbalance the probability for type 1 and type 2 statistical errors, an uncorrected $p < .05$ was considered significant. But for comparison reasons, corrected *p*-values

($_{FDR}p$) using the False-Discovery Rate (FDR; (Benjamini & Hochberg, 1995); hemisphere (2) x Y-BOCS-score (2)) are also reported if uncorrected values were considered significant.

2.3.4. LFP-study: Explorative anatomical analysis

An explorative anatomical analysis[1] was performed regarding the localization of the depth electrode contacts showing the highest expression of the LFP-correlates ΔLFP-conflict-theta, ΔLFP-error-theta and ΔLFP-ERN. DBS electrode location were reconstructed using the Lead-DBS toolbox (Horn & Kuhn, 2015; Horn, et al., 2019). First, pre-operative magnetic resonance imaging and postoperative computer tomography images were linearly coregistered using Advanced Normalization Tools (ANTs; (B. Avants, Tustison, & Song, 2008; B. B. Avants, Epstein, Grossman, & Gee, 2008; Schonecker, Kupsch, Kuhn, Schneider, & Hoffmann, 2009). Next, images were nonlinearly transformed into standard MNI space (ICBM 2009b NLIN Asym space, (Fonov, et al., 2011)). Locations of the DBS electrode were identified and reconstructed using PACER (Husch, M, Gemmar, Goncalves, & Hertel, 2018). If required, electrodes were manually refined and corrected for postoperative brain shift. The averaged values of LFP-correlates from each electrode contact were assigned to respective location using color-coded marker.

2.4. Stimulation-study

2.4.1. Stimulation-study: Data collection

Patients' data were acquired at three recording sessions (Figure 4). First session was performed before DBS surgery (pre). The second and third sessions were performed during the follow-up visit, at least 6 months after DBS surgery with active stimulation (on) and with discontinued stimulation between 12 - 24 hours (off). The order of the on and off measurements was assigned pseudo randomly. If the first follow-up session was measured in off, the on session was performed at least 24 hours after switching the stimulation on again. Of the 18 subjects, three did not attend one or both follow-up sessions because of concerns regarding cessation of stimulation or due to organizational reasons, such as conflicting schedules or personnel absence (Table 1) and are thus not included in the **Stimulation-study**.

[1] The explorative anatomical analysis was performed primarily by Dr. Thomas Schüller, University of Cologne, Faculty of Medicine and University Hospital Cologne, Department of Psychiatry and Psychotherapy, 50935 Cologne, Germany

All recordings took place in a dimly lit, electronically, and acoustically shielded room. Electrophysiological scalp data were recorded using 64-Channel 10-20 system Ag/AgCl caps (Easycap, Herrsching, Germany). All data were recorded at the sampling rate of 5000 Hz (BrainAmp MR plus amplifiers; Brain Products, Gilching, Germany) with impendences below 15 kΩ.

Patients' symptom severity was assessed before DBS surgery, at follow-up visit before the experimental sessions and at the end of the clinical study (at least 12 months after surgery) using the Y-BOCS.

2.4.2. Stimulation-study: Data analysis

Data were processed using EEGLAB 14.1.1 (Delorme & Makeig, 2004) and custom Matlab 2017a routines (The Math Works Inc., Natick, U.S.A.). All data were filtered with cut-off frequencies of 0.5 and 40Hz (6dB/Octave) using a phase free finite impulse response filter and resampled to 500 Hz. Additionally, DBS stimulation artifacts were removed by a custom Hampel filter by discarding spectral outliers in the frequency-domain (Allen, Stegemoller, Zadikoff, Rosenow, & Mackinnon, 2010).

Stimulus-locked epochs were extracted from -1500 ms to 3500 ms. To improve data quality, epochs exceeding 5 standard deviations of the joint data probability were discarded. Eye movements and pulse artifacts were removed using ICA (Makeig, et al., 2004) through manual identification of the respective independent components rejection (rejected ICs in sessions pre: 3.1±1; on: 1.7±0.9; off: 3.3±1). Data were re-referenced to linked mastoids.

All conflict-related analysis was performed on the stimulus-locked data in order to align the EEG activity on the stimulus presentation. Conflict-related theta- (conflict-theta) analysis was performed with incompatible and compatible correct trials, with the aim to observe merely the conflict effect and avoid influence from error-related processing.

Time-frequency decomposition was performed by convoluting data from single trials with Morlet wavelets: $e^{i2\pi tf}e^{-t^2/(2*\sigma^2)}$ where t is time, f is frequency, and σ specifies the width of each frequency band. f was set from 1 to 40 Hz and increased in 50 logarithmically spaced steps. σ was defined as $3.5/(2\pi f)$, where 3.5 specifies the number of wavelet cycles. Fast Fourier transform (FFT) was performed on the data and subsequently multiplied with the power spectrum of Morlet wavelets providing the power spectrum of the EEG data. Inverse FFT was applied resulting in complex signal. Out of this, frequency-specific power was defined as the value $Z(t) = \text{real}[z(t)]^2 + \text{imag}[z(t)]^2$). Power was normalized and baseline corrected using a

decibel (dB) transform (dB power(*tf*) = 10*log10[power(*tf*)/baseline]). The baseline power for conflict-theta-analysis was set from -300 to -100 ms before stimulus.

Mean conflict-theta power was calculated at electrode FCz from 3 to 7 Hz and 200 to 600 ms for each subject and condition (Cavanagh, et al., 2009). The conflict-effect (Δconflict-theta) was calculated by subtracting the mean of the compatible trials from the mean of the incompatible trials. In the following, conflict-theta is referred to as MFC-conflict-theta (effect as ΔMFC-conflict-theta).

All error- or accuracy-related analyses were performed on response-locked data in order to align the EEG activity on the response execution. Therefore, data were extracted from -1300 ms to 1500 ms relative to the response. The number of error trials in the low-conflict (compatible) condition was quite small in most of the patients (mean 9±9 trials) and thus insufficient for an adequate signal-to-noise ratio needed for a reliable EEG-analysis (Fischer, et al., 2017). Thus, only high conflict (incompatible) error and correct trials were included in the analysis.

For ERP-analysis, baseline correction was applied from -300 ms to -100 ms relative to stimulus onset and trials of each condition were averaged within subjects. ERN/CRN amplitudes were measured at electrode FCz. Since a trough-to-peak amplitude measure has been suggested as a baseline-independent measure (Falkenstein, et al., 2000; Kopp, et al., 1996), we used this approach (search window for peak: from 0 to 150 ms; search window for trough: from -100 ms to the peak).

In contrast to the **LFP-study**, in the **Stimulation-study** we refrained from error-related theta analysis due to following reasons. Since this study handles cortical and not striatal activity, we were primarily interested in the widely investigated error-related EEG activity that is comprised by the ERP-analysis. Further, the analysis of error-related theta activity in the **LFP-study** enabled the assessment of frontostriatal connectivity, that was not possible in the **Stimulation-**study, this analysis was therefore not valuable.

2.4.3. Stimulation-study: Statistical analysis

If not otherwise indicated, analyses were performed with repeated-measures analyses of variance (3 x 2 rmANOVA). For the analysis of conflict-related task performance, error rate of high-/low- conflict trials and RTs were analyzed with stimulation (pre, on, off) and compatibility (compatible, incompatible) as within subject factors. For the analysis of error-

related task performance, RTs were analyzed with stimulation (pre, on, off) and accuracy (error, correct) as within subject factors.

MFC-conflict-theta was analyzed with stimulation (pre, on, off) and compatibility (compatible, incompatible) as within-subject factors. The ERN/CRN was analyzed with within subject factors stimulation (pre, on, off) and accuracy (correct, error). Additionally, planned comparisons were performed for the ΔMFC-conflict-theta and the ERN (paired *t*-tests; pre vs. on, on vs. off, pre vs. off).

In all ANOVAs, if the assumption of sphericity was violated, the Greenhouse-Geissler correction was applied.

Spearman correlation was performed to test the relationship between the reduction of symptom severity at the end of the clinical study (in %; $Y\text{-}BOCS_{\%change}$) with EEG-correlates. Particularly, pre, pre-on, pre-off and on-off change for ERN and ΔMFC-conflict-theta were used for correlation. To counterbalance the probability for type 1 and type 2 statistical errors, an uncorrected $p < .05$ was considered significant. But for comparison reasons, corrected *p*-values ($_{FDR}p$) using FDR-correction (ΔMFC-conflict-theta/ERN variables (4) x Y-BOCS-score (1)) are also reported if uncorrected values were considered significant.

2.4.4. Stimulation-study: Explorative anatomical analysis

An explorative anatomical analysis[2] was performed regarding the location of DBS and its impact on changes in ΔMFC-conflict-theta, ERN, and Y-BOCS. DBS electrode location were reconstructed using the Lead-DBS toolbox (Horn & Kuhn, 2015; Horn, et al., 2019). First, pre-operative magnetic resonance imaging and postoperative computer tomography images were linearly coregistered using Advanced Normalization Tools (ANTs; (B. Avants, et al., 2008; B. B. Avants, et al., 2008; Schonecker, et al., 2009). Next, images were nonlinearly transformed into standard MNI space (ICBM 2009b NLIN Asym space, (Fonov, et al., 2011)). Locations of the DBS electrode were identified and reconstructed using PACER (Husch, et al., 2018). If required, electrodes were manually refined and corrected for postoperative brain shift. The stimulation volumes were estimated using FastField (Baniasadi, Proverbio, Goncalves, Hertel, & Husch, 2020). All stimulation volumes were nonlinearly transformed to the right hemisphere. Changes in ΔMFC-conflict-theta, ERN and Y-BOCS from pre to on were corrected

[2] The explorative anatomical analysis was performed primarily by Dr. Till A. Dembek, University of Cologne, Faculty of Medicine and University Hospital Cologne, Department of Neurology, 50935 Cologne, Germany

for stimulation amplitude. To create a mean-effect-image for each outcome the corrected variables were assigned to each voxel of the respective stimulation volume and averaged over all stimulation volumes (Dembek, et al., 2017). In order to facilitate comparability between outcomes, values in each mean-effect-image were z-transformed using their respective mean and standard deviation.

3. Results

3.1. LFP-study

3.1.1. LFP-study: Task performance

Error rate was higher in high-conflict (incompatible) than low-conflict (compatible) trials (compatible 3±1%, incompatible 11±1%; $t(13)=7.6$, $p<.001$), showing successful modulation of response tendencies by the flanker stimuli.

RTs of correct high-conflict trials were slower compared to correct low-conflict trials (compatible correct 370±11 ms, incompatible correct 436±13 ms; $t(13)=16.7$, $p<.001$; Figure 5) and also slower compared to error high-conflict trials (incompatible error 316±10 ms; $t(13)=26.1$, $p<.001$). This demonstrates the successful modulation of response tendencies and the response selection process by the flanker stimuli. High-conflict conditions thereby leaded to increased time to correctly resolve decision conflict, or to fast erroneous response if not enough time was granted for conflict resolution.

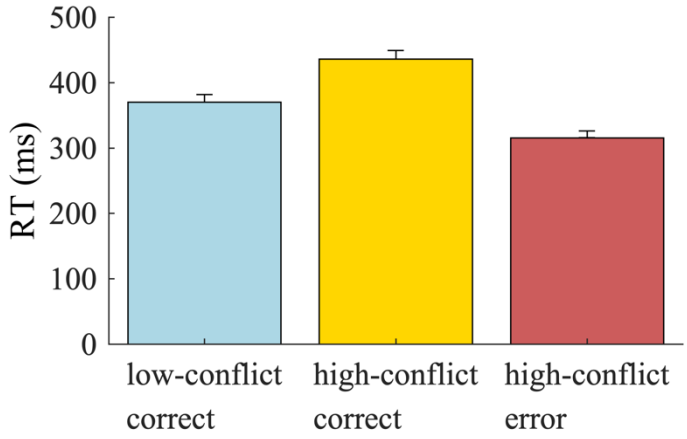

Figure 5 Reaction times during low- and high conflict trials. Depicted are means and SEM.

3.1.1. LFP-study: Electrophysiological results

Conflict-theta

MFC-conflict-theta was increased during high-conflict compared to low-conflict trials (compatible correct 0.7±0.3 dB, incompatible correct 1.6±0.5 dB; $t(13)=4.0$, $p=.002$; Figure 6), showing successful modulation of theta activity by conflict at scalp surface.

LFP-conflict-theta revealed a significant main effect of compatibility [$F(1,13)=8.5$, $p=.012$], signifying also increased LFP-conflict-theta in high-conflict compared to low-conflict

trials and thus successful modulation of theta by conflict in the ALIC/NAc (Figure 6). There was no significant main effect of hemisphere or interaction (all $p>.5$), indicating no differences in modulation between hemispheres.

There was no significant relationship between the $Y\text{-}BOCS_{pre}$ or $YBOCS_{\%change}$ and the ΔLFP-conflict-theta (all $p>.08$).

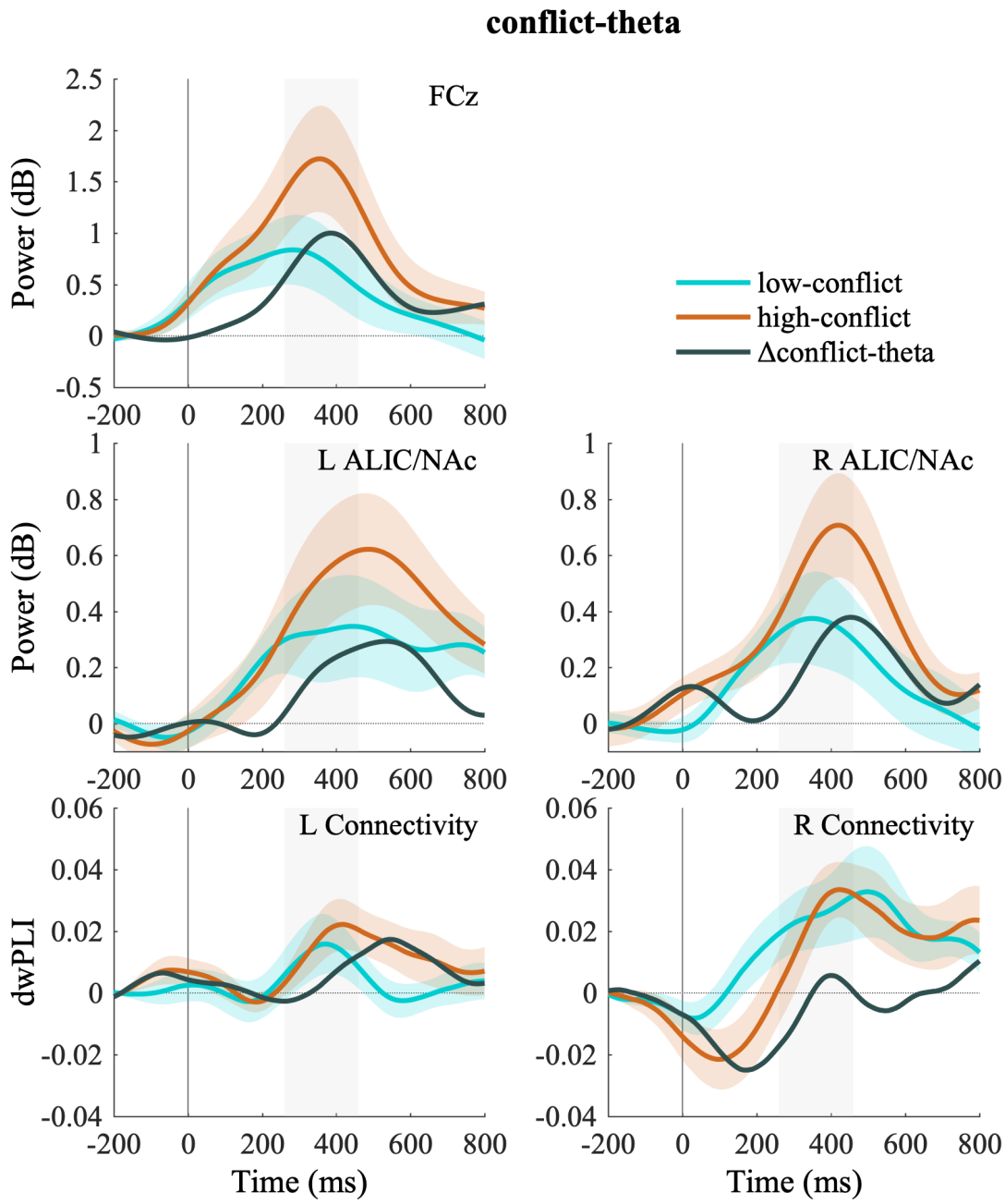

Figure 6 MFC-conflict-theta (top), LFP-conflict-theta in the left and right ALIC/NAc (middle) and their connectivity (bottom). Shaded area indicates time window for amplitude measure/statistical analysis. (Modified from Sildatke & Schüller, in preparation)

Analysis of frontostriatal connectivity at the time of conflict-theta revealed no significant main effect of hemisphere, compatibility or interaction (all $p>.3$; Figure 6), indicating the connectivity neither to differ between hemispheres nor to be modulated by conflict. Exploratory analyses indicated greater frontostriatal theta connectivity compared to baseline in high-conflict trials bilaterally (right: $t(13)=3.7$, $p=.003$; left $t(13)=2.7$, $p=.02$) and in low-conflict trials in the right hemisphere ($t(13)=2.5$, $p=.028$; left $t(13)=1.4$, $p=.18$). This indicates a presence of theta mediated frontostriatal connectivity, but absence of its modulations by the degree of the conflict.

There was no significant correlation between Δconflict-theta-connectivity and the $Y\text{-}BOCS_{pre}$ or $YBOCS_{\%change}$ (all $p>.18$), indicating no association between frontostriatal connectivity at the time of conflict-theta and the clinical score.

Error-theta

MFC-error-theta was increased in error compared to correct trials (incompatible correct 0.2±0.2 dB, incompatible error 2.3±0.5 dB; $t(13)=4.8$, $p<.001$; Figure 7), demonstrating successful modulation of theta activity by accuracy at scalp surface.

LFP-error-theta revealed a significant main effect of accuracy [$F(1,13)=5.2$, $p=.04$], showing increased LFP-error-theta in error compared to correct trials and also demonstrating successful modulation of theta activity in the ALIC/NAc. There was no significant main effect of hemisphere or interaction (all $p>.9$), indicating no differences in modulation between hemispheres.

The results indicated a significant positive relationship between $Y\text{-}BOCS_{pre}$ and the ΔLFP-error-theta in the left hemisphere ($r=-57$; $p=.035$; $_{FDR}p=.07$). This relationship associates patients with higher symptom severity with a greater error-induced theta modulation in the left hemispheric LFPs.

There was a significant negative relationship between $Y\text{-}BOCS_{\%change}$ and the ΔLFP-error-theta in the right hemisphere ($r=-.68$; $p=.01$; $_{FDR}p=.038$; Figure 9). This relationship associates patients with a smaller error-effect in the right LPF with a higher symptom improvement after DBS.

The analyses of frontostriatal connectivity at the time of error-theta indicated no significant main effect of hemisphere, accuracy or interaction (Figure 7, all $p>.097$), indicating the connectivity not to differ between hemispheres or to be modulated by accuracy. Exploratory analysis indicated greater frontostriatal theta connectivity compared to baseline in error trials in the right hemisphere ($t(13)=2.7$, $p=.019$; left $t(13)=1.7$, $p=.11$) and in correct trials bilaterally

(right: $t(13)=2.4$, $p=.035$; left $t(13)=2.6$, $p=.021$). This indicates a presence of theta mediated frontostriatal connectivity after the response, but absence of its modulations by accuracy.

The results indicated a significant negative relationship between Y-BOCS$_{\%change}$ and Δerror-theta-connectivity (Figure 10; r=-.74; $p=.004$; $_{FDR}p=.015$) limited to the right hemisphere. This relationship associates patients with increased frontostriatal connectivity following errors with attenuated DBS-induced symptom improvement.

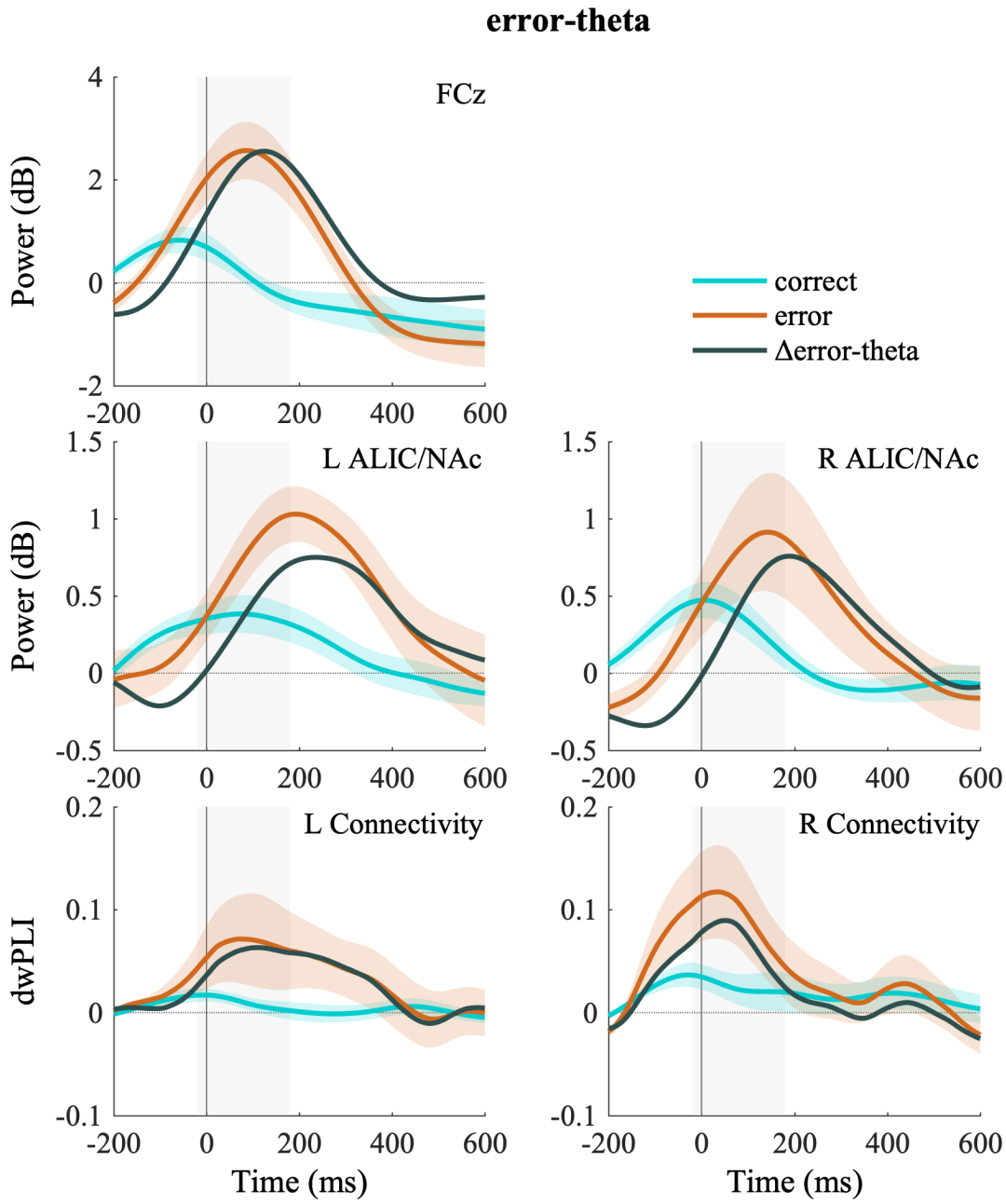

Figure 7 MFC-error-theta (top), LFP-error-theta in the left and right ALIC/NAc (middle) and their connectivity (bottom). Shaded area indicates time window for amplitude measure/statistical analysis. (Modified from Sildatke & Schüller, in preparation)

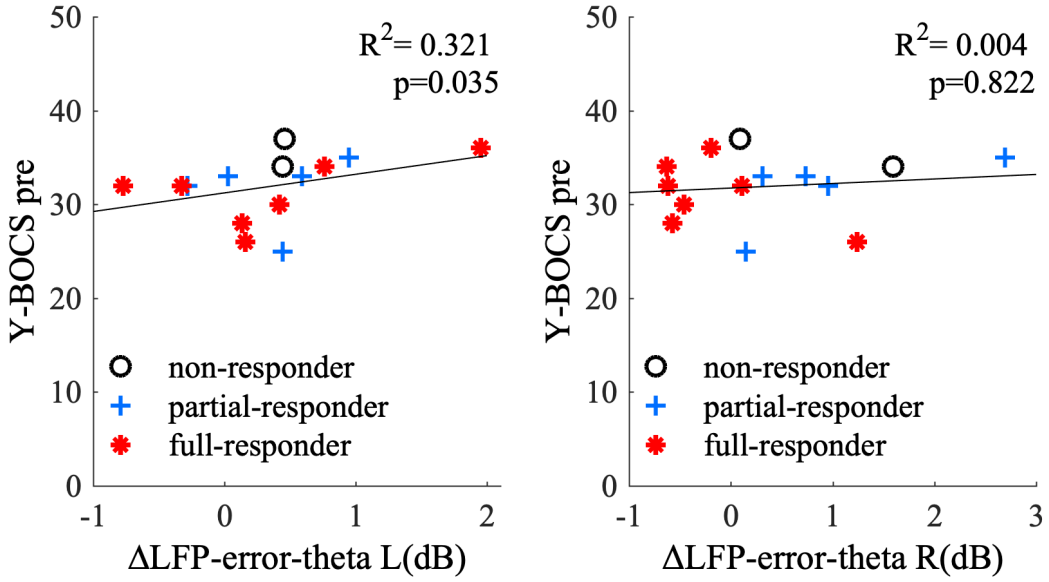

Figure 8 Correlation between the pre-operative symptom severity (Y-BOCS$_{pre}$) and ΔLFP-error-theta in the left and right ALIC/NAc. Score reduction of <25% =non-responder; 25-34% =partial-responder; ≥35% =full-responder. Indicated are uncorrected *p*-values. (Modified from Sildatke & Schüller, in preparation)

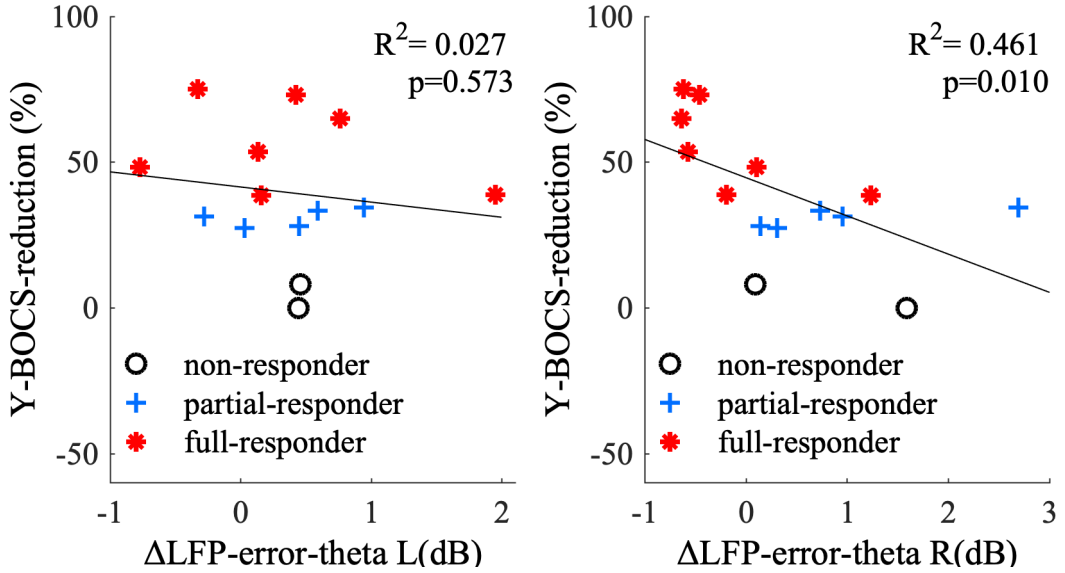

Figure 9 Correlation between the reduction of symptom severity (Y-BOCS$_{\%change}$) and ΔLFP-error-theta in the left and right ALIC/NAc. Score reduction of <25% =non-responder; 25-34% =partial-responder; ≥35% =full-responder. Indicated are uncorrected *p*-values. (Modified from Sildatke & Schüller, in preparation)

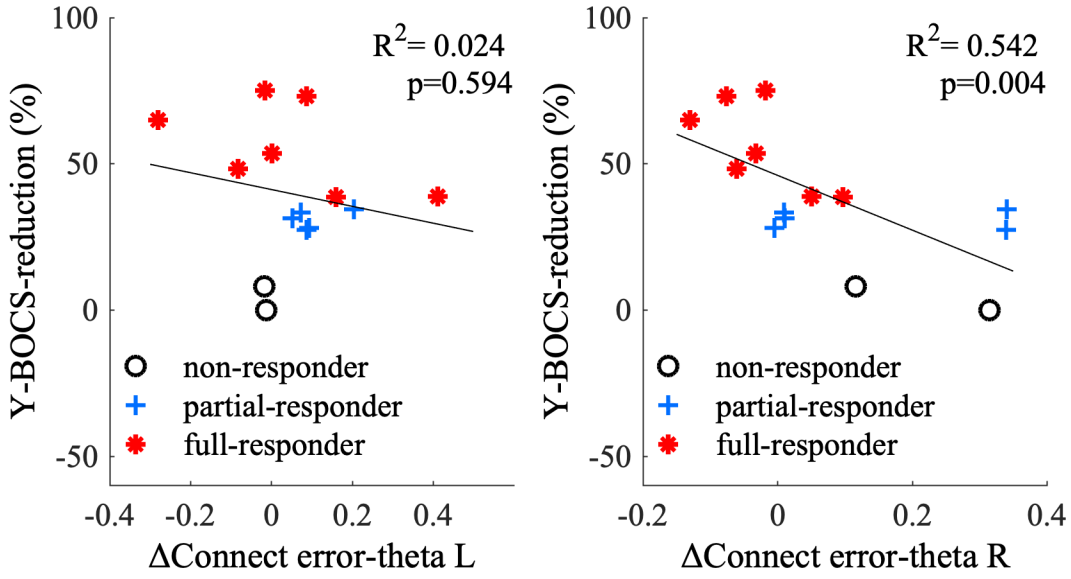

Figure 10 Correlation between the reduction of symptom severity (Y-BOCS$_{\%change}$) and error-theta-mediated frontostriatal connectivity-change (error – correct) in the left and right ALIC/NAc. Score reduction of <25% =non-responder; 25-34% =partial-responder; ≥35% =full-responder. Indicated are uncorrected *p*-values. (Modified from Sildatke & Schüller, in preparation)

ERPs

There was a significant ERN represented by a larger negative deflection in error compared to correct trials, (incompatible error -2.0±0.9 µV, incompatible correct 3.8±1.2 µV; $t(13)=3.0$, $p=.01$; Figure 11).

Likewise, in the LFPs there was a significant main effect of accuracy [incompatible error -0.8±1.8 µV, incompatible correct 0.8±1.1 µV; $F(1,13)=11.9$ $p=.004$], with larger deflections for error than correct trials (Figure 11). There was no significant main effect of hemisphere or interaction (all $p>.4$), indicating no differences in modulation between hemispheres.

There was a significant negative relationship between ΔLFP-ERN in the right hemisphere and Y-BOCS$_{pre}$ (r=-.71; $p=.004$; $_{FDR}p=.017$; Figure 12), indicating increased LFP error modulation to be associated with higher symptom severity. Further, there was at trend-level significant correlation between the error-effect in the right hemisphere and Y-BOCS$_{\%change}$ (r=.51; $p=.067$; $_{FDR}p=.13$ Figure 13).

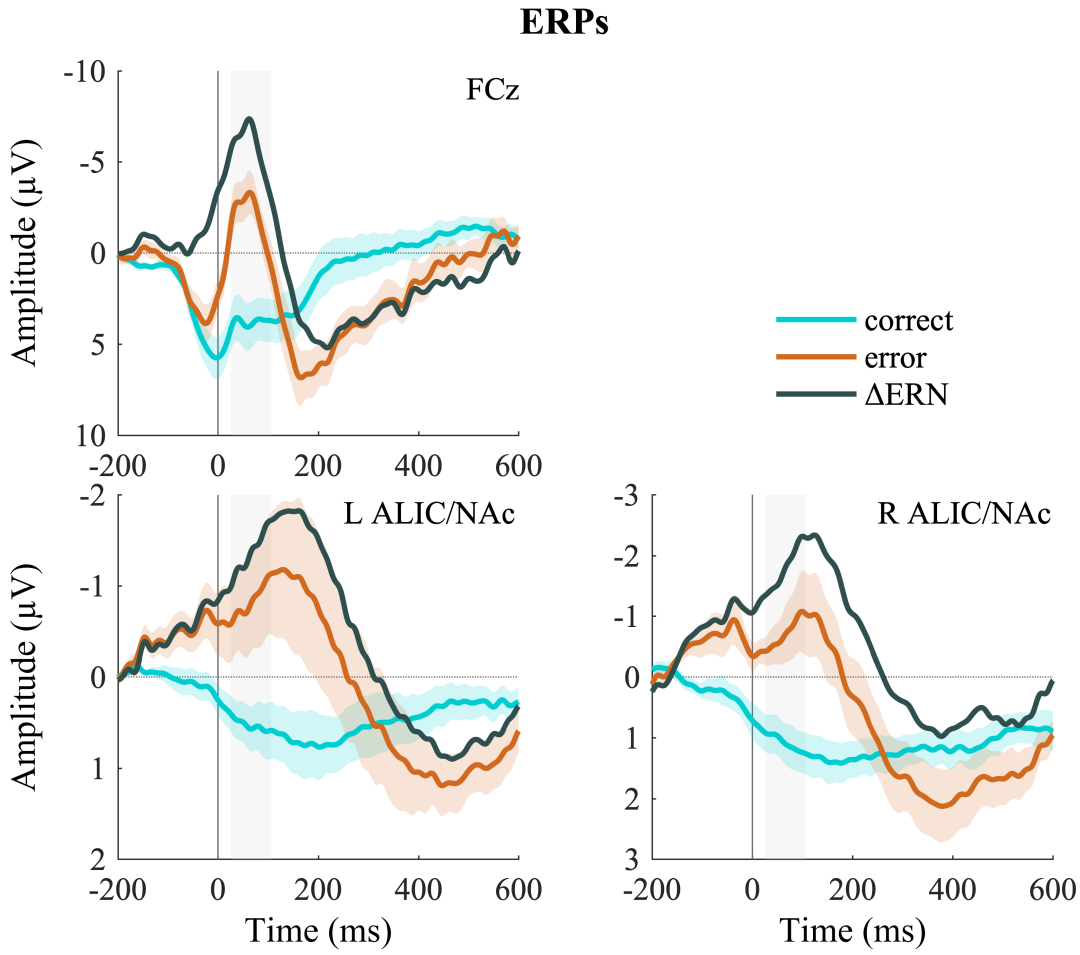

Figure 11 ERPs at FCz (top), in the left and right ALIC/NAc (bottom). Shaded area indicates time window for amplitude measure/statistical analysis.

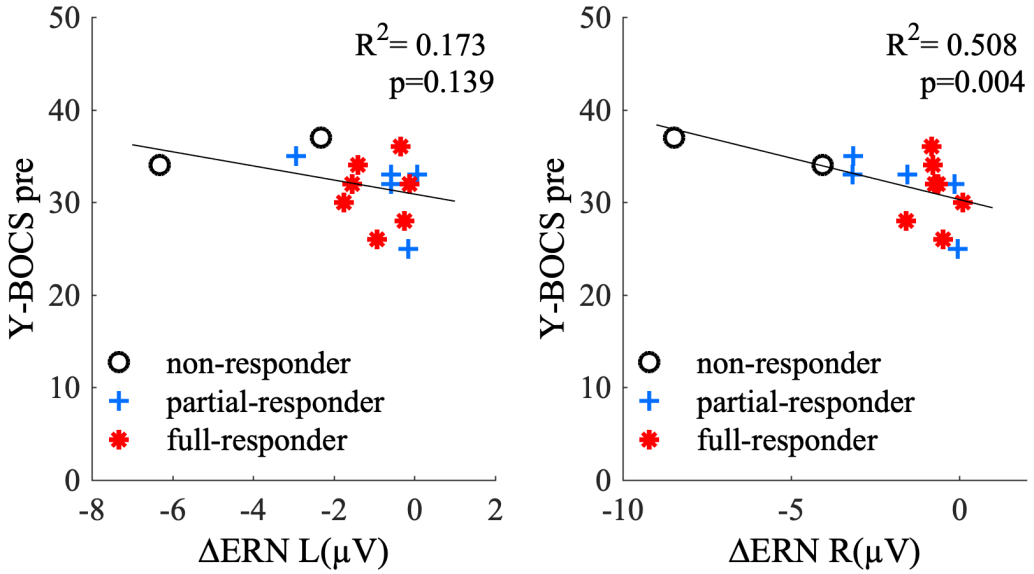

Figure 12 Correlation between pre-operative symptom severity (Y-BOCS$_{pre}$) and ΔLFP-ERN in the left and right ALIC/NAc. Note: more negative ΔLFP-ERN values indicate stronger error modulation. Score reduction of <25% =non-responder; 25-34% =partial-responder; ≥35% =full-responder. Indicated are uncorrected *p*-values.

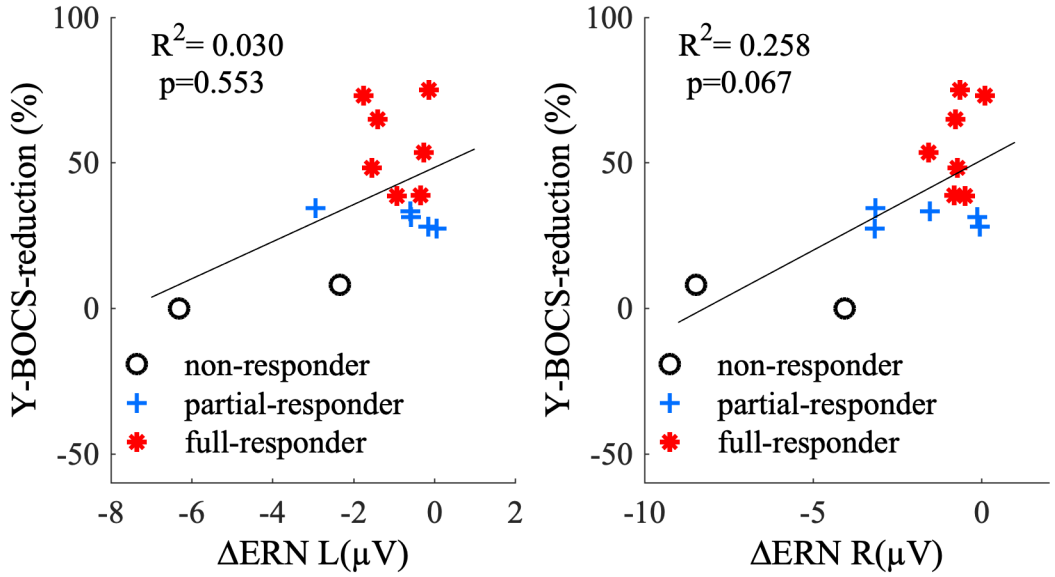

Figure 13 Correlation between the reduction of symptom severity (Y-BOCS$_{\%change}$) and ΔLFP-ERN in the left and right ALIC/NAc. Note: more negative ΔLFP-ERN values indicate stronger error modulation; Score reduction of <25% =non-responder; 25-34% =partial-responder; ≥35% =full-responder. Indicated are uncorrected *p*-values.

3.1.2. LFP-study: Exploratory anatomical analysis

Exploratory anatomical analyses indicated higher ΔLFP-conflict-theta, ΔLFP-error-theta and ΔLFP-ERN for electrode contacts located in and around NAc compared to contacts located more dorsally in the ALIC (Figure 14).

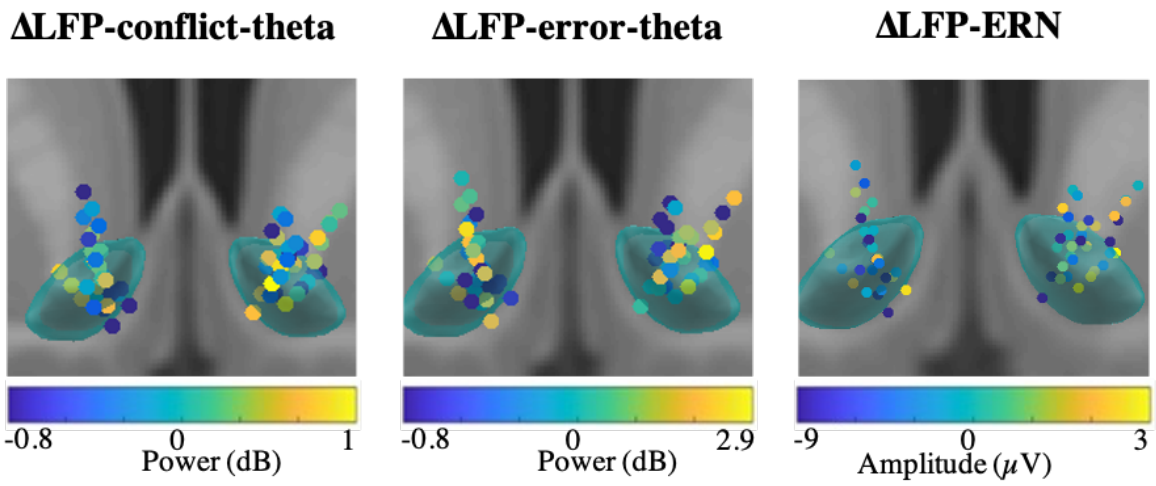

Figure 14 Expression of theta power on single electrode contacts within the ALIC/NAc region for ΔLFP-conflict-theta (left), ΔLFP-error-theta (middle) and ΔLFP-ERN (right). All measures were most pronounced inside and around the NAc (turquoise) than in the ALIC. Note: more negative ΔLFP-ERN values indicate stronger error modulation. The NAc was derived from CIT168 Reinforcement Learning Atlas (Pauli, Nili, & Tyszka, 2017) and a coronal section of the MNI template is shown at y =9mm.

3.2. Stimulation-study

3.2.1. Stimulation-study: Task performance

In the **Stimulation-study** a significant main effect of compatibility [F(1,14)=24.39, p<.001] indicated a higher error rate for high-conflict trials compared to low-conflict trials (Figure 15). There was no significant effect of stimulation [F(1.3,18)=0.64, p=.48] or interaction [F(1.5,20)=1.37, p=.27].

For conflict-related RT (compatible/incompatible correct), there was a significant main effect of compatibility [F(1,14)=340.54, *p*<.001; Figure 15], indicating slower RT in high-conflict compared to low-conflict trials and no significant effect of stimulation [F(1.4,20)=2.0, *p*=.17] or interaction [F(2,28)=.29, *p*=.75].

Analysis of error-related RT (incompatible error/correct) revealed a significant main effect of accuracy [F(1,14)=531.72, *p*<.001] and a significant main effect of stimulation [F(2,28)=4.17, *p*=.026] and no significant interaction [F(2,28)=.68, *p*=.52]. RTs were slower in correct than in error trials (Figure 15) and slower in off (436.4 ± 19.4ms) than in pre (420.8 ± 12.8 ms) or on (420.3 ± 15.3 ms) although no significant difference was revealed by planned comparisons (pre vs. on: *p*=.95; pre vs. off: *p*=.13; on vs. off: *p*=.11).

3.2.1. Stimulation-study: Electrophysiological results

Conflict-theta

MFC-conflict-theta was increased in high-conflict compared to low-conflict trials as indicated by a significant main effect of compatibility [F(1,14)=35.44, *p*<.001]. There was no significant main effect of stimulation [F(2,28)=1.76, *p*=.19]. There was a significant interaction of stimulation and compatibility [F(2,28)=3.43, *p*=.047], but post-hoc test revealed no significant results (all $_{FDR}$-*p*>.07). Planned comparisons indicated decreased ΔMFC-conflict-theta in on than in pre (*t*(14)=-2.3, *p*=.034; $_{FDR}$-*p*=.1; Figure 16A) with no significant differences between pre and off (*p*=.278) and on and off (*p*=.107).

There was no significant relationship of the Y-BOCS$_{\%change}$ with the ΔMFC-conflict-theta (pre: *p*=.37; pre-on: *p*=.49; pre-off: *p*=.90; on-off: *p*=.60).

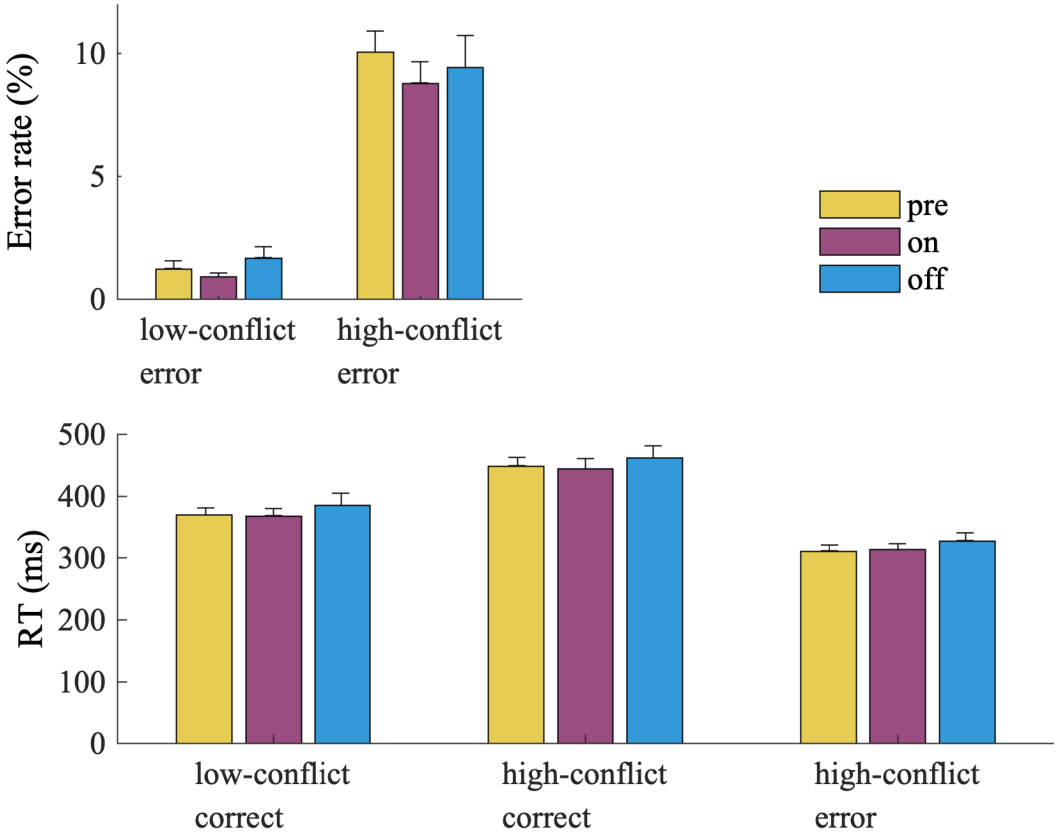

Figure 15 Task performance results. Error rate (top) in low-conflict (compatible) and high-conflict (incompatible) trails and RT (bottom) during the pre, on and off session. Depicted are means and SEM. Modified after Sildatke, et al. (2021)

ERP

The ERP-analysis revealed a main effect of accuracy [$F(1,14)=17.08$, $p=.001$] and a main effect of stimulation [$F(1.2,16.5)=4.48$, $p=.045$], the former indicating increased amplitude in error than correct trials. There was no significant interaction between stimulation and accuracy ($p=.45$). Planned comparisons indicated decreased ERN amplitude in on than in pre session ($t(14)=-5.11$, $p<.001$; $_{FDR}p<.001$) and at trend-level decreased ERN in on than in off session ($t(14)=-2.12$, $p=.052$; $_{FDR}p=.078$; Figure 16B). There was no significant difference between ERN in pre and off sessions ($t(14)=0.63$, $p=.54$). Because the investigation of the CRN was not part of this study, no planned comparisons were performed. Generally, the stimulation-induced changes on CRN amplitude resembled those of the ERN (Figure 17).

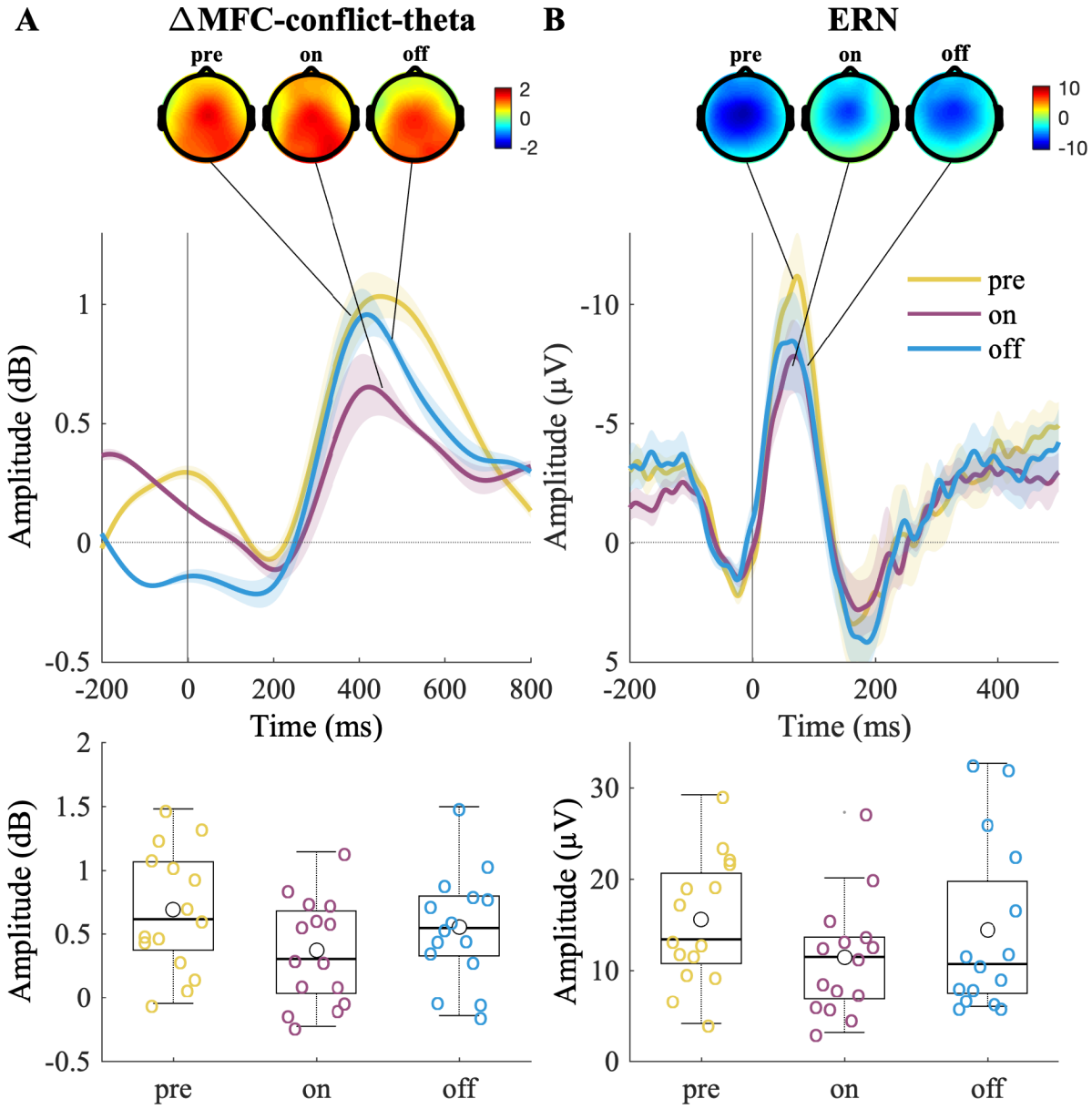

Figure 16 Conflict-related (ΔMFC-conflict-theta) and error-related (ERN) electrophysiological results during the pre, on and off session. A) Top: Topographic maps of theta activity during conflict (incompatible correct trials; 3-7 Hz; 200-600 ms). Middle: Waveforms of ΔMFC-conflict-theta activity. Bottom: Boxplots for ΔMFC-conflict-theta. Colored circles represent means of individual patients. B) Top: Topographic maps of activity (error-correct trials) at the time of grand-average peak. Middle: Waveforms of ERN activity following error trials. A response-locked baseline (-200 ms to -100 ms) was applied to data for visualization. Bottom: Boxplots for ERN amplitudes (trough-to-peak measure). Colored circles represent means of individual patients. Modified from Sildatke, et al. (2021)

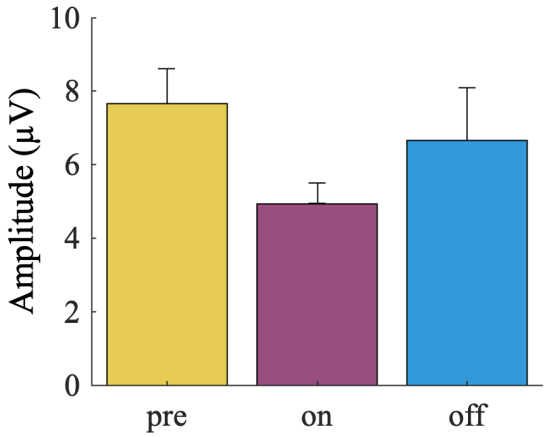

Figure 17 CRN (trough-to-peak measure) during the pre, on and off session. Depicted are means and SEM. Adapted from Sildatke, et al. (2021)

We found a significant negative correlation between Y-BOCS$_{\%change}$ and the pre ERN (r=-.70; p=.0049; $_{FDR}$-p=.02; Figure 18), indicating smaller pre ERN to be related to increased symptom improvement. We found no significant relationship between Y-BOCS$_{\%change}$ and the ERN change between sessions (pre-on: p=.13; pre-off: p=.89; on-off: p=.46).

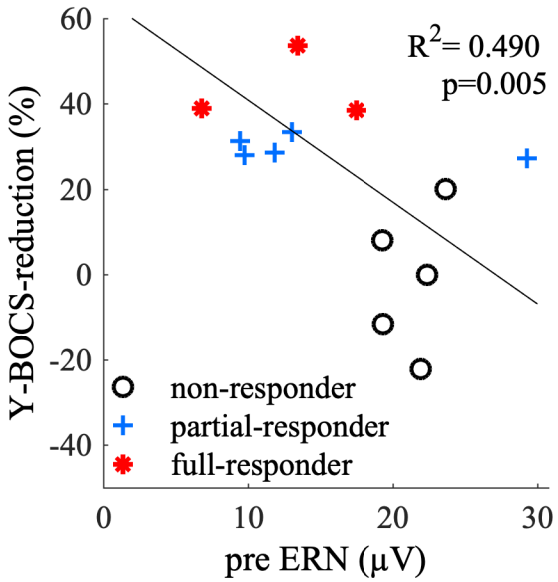

Figure 18 Correlation between the reduction of symptom severity (Y-BOCS$_{\%change}$) and pre ERN (trough-to-peak measure) after at least 12 months of stimulation. Note: more positive ERN values indicate stronger error modulation. Score reduction of <25% =non-responder; 25-34% =partial-responder; ≥35% =full-responder. Indicated are uncorrected p-values. Modified from Sildatke, et al. (2021)

3.2.2. Stimulation-study: Exploratory anatomical analysis

Images of exploratory anatomical analysis indicated a ventral-dorsal gradient of the DBS mean-effect for ΔMFC-conflict-theta, ERN, and Y-BOCS (Figure 19). ERN and Y-BOCS reductions from pre to on were greatest in patients with stimulation located more dorsally in the ALIC. Surprisingly, ΔMFC-conflict-theta reduction from pre to on indicated an opposite gradient, that was lowest in the ALIC and instead more pronounced by stimulation in and around the NAc.

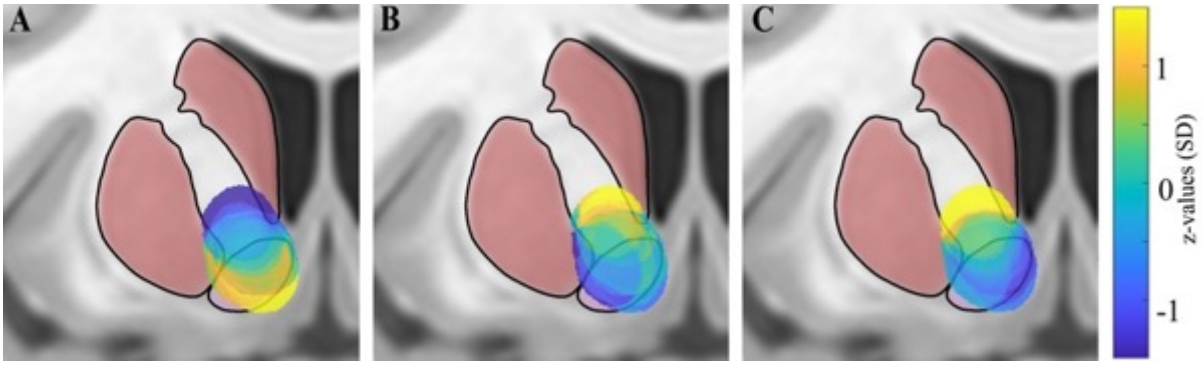

Figure 19 Mean-effect-images for A) ΔMFC-conflict-theta, B) ERN, and C) Y-BOCS showing changes from pre to on. While reduction of ΔMFC-conflict-theta was most pronounced ventrally, inside and around the NAc (pink), reduction of ERN and Y-BOCS was most pronounced in the ALIC. The striatum (dark red) and NAc (pink) were derived from CIT168 Reinforcement Learning Atlas (Pauli, et al., 2017) and a coronal section of the MNI template is shown at y = 8mm. Values in the mean-effect-images were z-transformed to a mean of 0 and a standard deviation of 1. Adapted from Sildatke, et al. (2021)

4. Discussion

4.1. Summary of the study results

Although ALIC/NAc is a prominent target region for DBS in OCD the knowledge regarding its involvement in performance monitoring and the effect of ALIC/NAc DBS on performance monitoring correlates is still limited.

The first aim of this dissertation is therefore the investigation of ALIC/NAc involvement in decision conflict and error-related processes, that are specifically represented by conflict-theta, error-theta and ERN (**LFP-study**). Behavioral results indicated that task manipulations were successful, with expected adaptation of behavior to decision conflict, including erroneous responses. In line with our hypotheses, cortical activity showed theta frequency modulations by decision conflict (high-conflict > low-conflict; hypothesis 1.1) and error processing (error > correct; hypothesis 1.3). As hypothesized, similar modulations by decision conflict (hypothesis 1.2) and error processing (hypothesis 1.4) were observed in the ALIC/NAc. As expected, investigation of the ERPs revealed increased ERN amplitude compared to CRN amplitude (hypothesis 1.5). This finding extended also to ERN/CRN-like modulations in the ALIC/NAc region, supporting our hypothesis (1.6). Contrary to our hypotheses (1.7 and 1.8), we found no increased modulations of corticostriatal connectivity for high-conflict and error trials, respectively. Furthermore, we explored interrelations between symptom severity (Y-BOCS$_{pre}$)/ symptom improvement after DBS (Y-BOCS$_{\%change}$) with conflict- and error-related activity in the ALIC/NAc, as described in the following. We found no interrelation between LFP-conflict-theta and symptom severity (hypothesis 1.9) or symptom improvement after DBS (hypothesis 1.14). We also found no interrelation between functional frontostriatal connectivity during conflict monitoring and the symptom scores (hypotheses 1.12 and 1.17). For error-related ALIC/NAc activity, we observed interrelations between symptom severity and LFP-error-theta (hypothesis 1.10) and LFP-ERN (hypothesis 1.11), respectively. Additionally, we found a negative interrelation between symptom improvement after DBS and LFP-error-theta (hypothesis 1.15) and LFP-ERN (at trend level; hypothesis 1.16). While functional frontostriatal connectivity during error processing was not interrelated with the symptom severity (hypothesis 1.13), we found a negative interrelation with symptom improvement after DBS (hypothesis 1.18). Finally, the distribution of ALIC/NAc activity was in line with ventral striatal sources of theta and ERP activity.

The second aim of this dissertation is the modulation of decision conflict and error processes by clinically effective ALIC/NAc stimulation in OCD patients (**Stimulation-study**).

Accordingly, we investigated MFC-conflict-theta and the ERN during three sessions: before DBS implantation (pre), and at follow-up with stimulation on and off. Behavioral results again indicated successful task manipulation of participants' behavior by response conflict. In line with our hypotheses, we found MFC-conflict-theta and the ERN to be modulated by DBS. Specifically, we observed decreased EEG modulations during stimulation on compared to pre (hypotheses 2.1 and 2.3). Contrary to our hypotheses, we found no significant increase of EEG modulations during stimulation on compared to off for the MFC-conflict-theta (hypothesis 2.2) and only a tendency for the ERN (hypothesis 2.4), implicating an acute effect of DBS. Furthermore, we found a negative interrelation between the symptom improvement after DBS and the pre ERN (hypothesis 2.6), but no interrelations with pre MFC-conflict-theta (hypothesis 2.5). We found also no interrelations between the symptom improvement after DBS and EEG changes induces by DBS (hypotheses 2.7 and 2.8). Finally, exploratory anatomical analyses indicated that DBS effects were related to NAc-stimulation for ΔMFC-conflict-theta and to ALIC-stimulation for ERN and symptom improvement after DBS.

4.2. Correlates of performance monitoring in the MFC and ALIC/NAc

Conflict detection and error processing are crucial features of performance monitoring during goal-directed behavior. The detection of conflict between competing response tendencies is the necessary first step in order to implement cognitive control to resolve conflict effectively. Likewise, after incorrect performance increased cognitive control is also required to initiate behavioral adaptations to improve future performance. The engagement of cognitive control is reflected by theta power increases in the MFC (Cavanagh, et al., 2012; Luu, et al., 2004; Trujillo & Allen, 2007). Correspondingly, in the present studies high conflict trials and performance errors robustly showed enhanced medial frontal increases in theta power, emphasizing raised control demands that were reflected in behavioral adaptation (i.e. longer reaction times in high conflict trials). Also, the ERN, a phase-locked theta signal (Trujillo & Allen, 2007), was reliably increased after performance errors. Therefore, the cortical modulation in response to increased cognitive control demands were expectedly in line with previous reports (Cavanagh, et al., 2012; Danielmeier, et al., 2009; Riesel, et al., 2014).

Furthermore, we observed corresponding theta modulations in response to performance errors in the ALIC/NAc, supporting findings of increased error-theta following failed motor inhibition (Eijsker, et al., 2020). Regarding the ERN modulation in the ALIC/NAc our finding is well in line with striatal LFP error modulations previously reported in a single patient with

OCD (Munte, et al., 2007), in four patients with severe alcohol abuse disorder (Heinze, et al., 2009; Voges, et al., 2013) and in four patients with severe opioid abuse disorder (Sildatke, et al., 2020). To the best of our knowledge, we are the first to show ALIC/NAc conflict modulation, highlighting the relevance in the performance monitoring network. The anatomical distribution of ALIC/NAc modulations pointed to a ventral striatal source but because of relatively sparse electrode arrays and limited sample size this observation needs to be interpreted with caution. Accordingly, our study provides additional insights regarding the involvement of the ALIC/NAc in performance monitoring processes that contribute to goal-directed behavioral adaptations.

4.3. Frontostriatal connectivity during conflict monitoring error processing

Increased frontostriatal communication via theta-band modulation has been reported for cognitive control to enable goal-directed behavior (Cohen, et al., 2012; Horschig, et al., 2015), reward processing (Cohen, et al., 2009c), reward anticipation (Cohen, et al., 2012) and motor inhibition (Eijsker, et al., 2020). The communication between the striatum and MFC is assumed to convey relevant stimulus information for subsequent behavioral adaptation (Eijsker, et al., 2020; Frank, Loughry, & O'Reilly, 2001; Horschig, et al., 2015). In line with this notion, frontostriatal connectivity represents a top-down signal to implement cognitive control (Cohen, et al., 2012; Horschig, et al., 2015). Against our expectations, theta modulations by conflict or errors were not accompanied by changes in frontostriatal connectivity. This could suggest the absence of direct interrelation between MFC and ALIC/NAc performance monitoring signals. Alternatively, communication is not mediated by the means of phase-synchronization as employed in this study. For example, phase-amplitude coupling constitutes a different mechanistic for interregional communication that should be explored in future studies. Also, our results are limited by the relatively small sample size and small to medium effects might have been missed (see section 4.6). Lastly, also specific task-demands might play an important role, as an interrelation of conflict-theta and NAc has been observed in OCD (Eijsker, et al. (2020). Nonetheless, communication between MFC and ALIC/NAc was apparent in our study, albeit not modulated by task conditions. Speculatively, the lack of condition differences was mediated by OCD related frontostriatal hyperconnectivity in situations where no increases of cognitive control are needed (i.e. low-conflict trials and correct responses). Overall, we conclude that frontostriatal communication is an integral element of the performance

monitoring network, but further research is needed to explore the electrophysiological mechanisms, signal-to-noise ratios and impact of the psychiatric disorder.

4.4. ALIC/NAc DBS modulates correlates of performance monitoring in the MFC

Next, we assessed the influence of clinically effective DBS on the cortical performance monitoring correlates. In line with our predictions, we found the MFC-conflict-theta and the ERN attenuated during stimulation in comparison to pre-operative state. First, in view of unchanged conflict adaptation in task behavior, reduction of MFC-conflict-theta likely reflects a decline in cognitive control demands without dropping the demands beyond the level of adequate performance ((Cavanagh, et al., 2012; Luu, et al., 2004). One can speculate, that this is achieved through improved signal-to-noise levels rendering a reduced signal sufficient for continual behavioral adaptation. Although these results need to be interpreted with caution, our exploratory anatomical analysis indicated that the modulation of MFC-conflict-theta was induced by affecting NAc rather than by modulation of hyperdirect pathway fibers in the ALIC. Consequently, we conclude that the modulation of MFC-conflict-theta reflects rather the monitoring of decision conflict than the subsequent behavioral adjustments, which are mediated by theta modulations conveyed by hyperdirect pathway fibers (Cavanagh, et al., 2011; B. Zavala, et al., 2013; B. A. Zavala, et al., 2014). Accordingly, the decrease of MFC-conflict-theta by stimulation likely reflects a downregulation of the overactive performance monitoring system in OCD.

In contrast to our study, Widge, et al. (2019) reported on increased theta power during striatal DBS that correlated with antidepressant effect in a sample of patients mainly exhibiting major depressive disorder. Speculatively, these contradictory findings might relate to disorder specific characteristics of ALIC/NAc DBS. However, a direct comparison of both studies is limited on account of differences in behavioral tasks and analyses methodology.

Second, the stimulation-induced reduction of the ERN can likewise be interpreted as successful modulation of an overactive performance monitoring system. Again, this modulation apparently exhibits an adaptive nature, as it does not affect task-related behavior, since error rates and RTs were unaltered. This is consistent with previous reports regarding normal-range behavioral performance in OCD irrespective of ERN amplitude alterations (Endrass & Ullsperger, 2014). Although our hypothesis was focused on the ERN it should be noted that stimulation equally modulated the CRN, the EEG responses in correct trials. Endrass, et al. (2008) reported increased CRN in OCD and, concurrent to the ERN, inferred this increase to

represent an overall hyperactive performance monitoring system. In accordance with this notion, our results indicate that DBS modulated broader performance monitoring processes, and not merely error-related processing.

Our exploratory anatomic analyses indicated that alterations of symptom severity and ERN were linked to largely overlapping fibers in the ALIC. The former is consistent with recent reports on clinical efficacy of ALIC/NAc DBS in OCD, showing a particular relationship with the stimulation of central ALIC fibers (Baldermann, et al., 2019; Li, et al., 2020). Furthermore, because this fiber bundle connects key-structures of the performance monitoring system (i.e. MFC, STN and thalamus; (Ullsperger, Danielmeier, et al., 2014)) it is conceivable that ALIC stimulation induced ERN changes as part of modulating a broader performance monitoring network. Nevertheless, observations from the exploratory anatomic analysis need to be considered preliminary and further research is necessary to elucidate the degree of circuits-overlap in the ALIC involving ERN and OCD symptom modulation.

Contrary to our hypothesis, cessation of stimulation led not to the expected recovery of EEG-correlates to the pre-operative state. Although, we observed a numerical shift towards the pre-operative state, with intermediate MFC-conflict-theta and ERN amplitudes during the off state, this effect was not significantly separable from the DBS-on states. Still, the numerically smaller gap between pre and off recordings might point towards a recovery of MFC-conflict-theta and ERN to pre-operative levels. Putatively, the period of discontinued stimulation was too short for a sufficient rebound. Likewise, in a study with patients with substance use disorder DBS restored the attenuated ERN that decreased again towards initial level after stimulation cessation (Kuhn, et al., 2011). While a systematic extension of the discontinuation period would be desirable to test these effects, patients' wellbeing is a very important factor and stress induced by the discontinuation of effective treatment should be limited to a tolerable minimum. In sum, DBS-induced reduction of MFC-conflict-theta and ERN can possibly be explained by acute effects on the performance monitoring network in OCD with additional research needed to further explore the timescales of DBS-induced modulations.

4.5. Interrelation between EEG-correlates and clinical scores

Another important aspect of this investigation of the performance monitoring system and its modulation by ALIC/NAc DBS constitutes the interrelation with OCD symptom severity and clinical efficacy. First, no interrelations between decision conflict modulations were found with symptom severity or clinical efficacy. Of course, a possible explanation would

be that conflict processing and OCD are in fact unrelated. Yet, there is evidence for a relationship between conflict processing and OCD. First, conflict related impairments might not be sufficiently reflected by Y-BOCS scores (Riesel, et al., 2017). Second, impairment in conflict processing in OCD is specifically observed in situation with high uncertainty (Mandali, Weidacker, Kim, & Voon, 2019) which might not extend to the flanker task. Yet again the limited statistical power of our sample might have precluded possible interrelation (see also section 4.6). The stimulation-induced changes in MFC-conflict-theta were also unrelated to clinical efficacy, while there is evidence that ALIC/NAc influences the cognitive control system implicated in conflict regulation (Li, et al., 2020; Widge, et al., 2019). Therefore, and additional to the points mentioned above, the specific requirements of the flanker task are important to consider. The elicited motor conflict might be differentially mediated than the more abstract decision conflict generally observed in obsessions (Shephard, et al., 2021). Particularly from a clinical perspective, the modulation of pathologically overactive control mechanisms provides a crucial mechanism of action of DBS in OCD. Importantly, this has been conceptualized to enable successful cognitive behavioral therapy for previously treatment-resistant OCD patients (Denys, et al., 2010). Overall, the idea that the modulation of cognitive control in the face of decision conflict might be an important mediator of clinical efficacy should not be dismissed prematurely, even though there was no additional evidence provided by this sample.

In contrast, cortical and striatal error processing modulations showed close association with symptom severity and clinical efficacy. The ERN is considered as a candidate endophenotype for OCD that is independent of clinical symptoms (Hajcak, et al., 2008; Riesel, et al., 2011; Riesel, et al., 2014). In line with the notion that effective treatment in OCD patients is generally not accompanied by cortical ERN modulations (Hajcak, et al., 2008; Riesel, et al., 2011; Riesel, et al., 2014) DBS-induced modulations of the ERN were unrelated to clinical success in our study. In contrast, larger pre-operative ERN amplitudes were predictive of reduced clinical efficacy. Thus, a consideration of the cortical ERN as a possible predictor for DBS patient selection could prove valuable, particularly since specific clinical predictors have not been identified so far (Alonso, et al., 2015; Huys, et al., 2019). Importantly, given limitations of the present study these results need to be considered preliminary and warrant further investigation.

Recent theories of OCD pathophysiology have emphasized the importance of frontostriatal hyperactivity. Yet, little is known about the interrelations of the performance monitoring system and OCD symptomatology. To the best of our knowledge, we provide the first insights in such association. Precisely, bilaterally increased ALIC/NAc error-modulation

was associated with increased symptom severity. Also, increased right lateralized ALIC/NAc error modulations were associated with diminished clinical efficacy of DBS. Together, these observations point toward a hyperactive striatal performance monitoring system related to symptom severity in OCD (Milad & Rauch, 2012) that is also related to attenuated clinical efficacy. Seemingly, the higher the expression of the error-related striatal activity, the more severe is the clinical impairment and the more difficult is it to restore the disease-related networks by DBS. Importantly, the limitations of our study have to be fully considered (section 4.6), and further research is needed to confirm those findings. Confirmation these preliminary results provided, striatal error-modulations could be an important candidate for a biomarker for the symptom state in OCD. In line with this notion, theta activity in the STN has been proposed as a biomarker for OCD (Rappel, et al., 2018). For example, a reliable subcortical biomarker could be used in the future to adapt stimulation settings or guide closed-loop DBS. Closed-loop entails feedback-controlled DBS by using predefined intracranial signals to regulate the application of DBS, a method that already finds successful application in epilepsy and movement disorders (Lo & Widge, 2017). In the future, long-term assessment of LFPs made available by the newest generation of stimulators might provide important insights in this regard. In that respect, future studies examining DBS-induced changes on error-related LFPs in the ALIC/NAc would be of special interest and could further strengthen the link between the performance monitoring system and symptom manifestation in OCD. Furthermore, patients of our study showed reduced symptom improvement related to increased frontostriatal connectivity. This finding might in turn be related to frontostriatal hyperconnectivity in OCD (Milad & Rauch, 2012; van den Heuvel, et al., 2016). Speculatively, this excessive frontostriatal connectivity might be associated with alterations in OCD-related networks that are not effectively modulated by ALIC/NAc DBS. However, it is important to note that connectivity was not significantly modulated by accuracy. Therefore it remains unclear, to which specific function the frontostriatal connectivity can be attributed. Surely, because of the given limitations (section 4.6), observations regarding clinical interrelations should rather be regarded as potential directors for further investigations. Nevertheless, these results might be a starting point of great value for future research and subsequent clinical application. Importantly, a cortical marker, as the ERN, could more easily find broader application, as the measurement is non-invasive and straightforward. Nonetheless, one should also take into account that enhancement of the ERN is not restricted to OCD but has been observed in anxiety disorders and depression (Riesel, 2019), suggesting this potential, if at all, to act as a complemented rather than stand-alone predictor. On the other hand, LFP-error-theta and corresponding connectivity

metrics, as well as the LFP-ERN can only be obtained from patients receiving surgery or that are already implanted with a DBS system that also enables long-term LFP recording. In conclusion, these results provide important insights in the relationship between the performance monitoring system and OCD symptomatology.

4.6. Limitations

This dissertation significantly contributes to the knowledge of ALIC/NAc involvement in performance monitoring processes and modulation of associated cortical correlates by DBS. However, the studies conducted for this dissertation have some limitations that need to be considered.

First, the relative low number of participants limits statistical power in both studies. Especially, the exploratory anatomical analyses require a larger sample to perform statistical testing and therefore remain descriptive. Also, planned comparisons were not corrected for multiple comparisons, but strictly limited to contrasts relating to the main hypotheses to prevent false positive findings. One should also keep in mind that due to the small sample size additional analyses of subgroups e.g., responder vs. non-responder, was not possible. Future studies with large sample sizes may be able to include those analyses that possibly provide further insights. Nevertheless, considering that patients with severe and otherwise treatment-refractory OCD who received DBS implantation were included in the studies, the number of participants can be regarded as rather large and the dropout rate due to post-operative fatigue (**LFP-study**) or fear of symptom relapse (**Stimulation-study**) can be regarded as rather low. While implementation of such complex studies is desirably, it is very difficult to achieve. Ideally, collaboration between different DBS centers could provide a feasible solution.

Second, comorbidities of our participants (Table 1, see also Huys, et al. (2019)), that are commonly observed in OCD (Endrass & Ullsperger, 2014) may have had an influence on the results.

Third, patients were treated with psychotropic medication. While selective serotonin reuptake inhibitors (SSRI) have no influence on the ERN in healthy subjects or OCD patients (Endrass & Ullsperger, 2014), benzodiazepines are known to reduce the ERN (de Bruijn, Hulstijn, Verkes, Ruigt, & Sabbe, 2004), but see Stern, et al. (2010) and Riesel, et al. (2015) for absent differences between medicated and unmedicated patients. Of note, medication was not stable between pre- and follow-up sessions. Accordingly, we cannot rule out medication

influences on our results. Further studies with stable medication are desirable, although difficult to implement considering the importance of the patients' wellbeing.

Fourth, the sessions in the **LFP-study** were conducted 1-2 days following DBS surgery and resulting fatigue may have had an effect on behavioral performance.

Fifth, the precise source of signal recorded by the LFPs cannot be determined. On the one hand, bipolar referencing provides a fairly local signal, cancelling out volume conducted sources. On the other hand, the limited number of electrode contacts and participants does not allow a reliable localization of the putative source of the signal. However, all electrodes were implanted within the ALIC/NAc region, as it was confirmed by postoperative imaging. Since activity measured by LFPs can extend several millimeters, we cannot conclude whether the measured signal exclusively represent activity from the ALIC/NAc region (Lempka & McIntyre, 2013). Still, no systematic differences in the LFPs in relation to their anatomical position could be detected.

Sixth, in the **Stimulation-study**, the time of ongoing stimulation (between 6 and at least 12 months) and the length of stimulation interruption (12-24 h) were heterogeneous between patients. This might also be a confounding factor. Especially, longer stimulation might potentially be accompanied by stronger effects on performance monitoring, i.e. further decrease of ERN and ΔMFC-conflict-theta during stimulation, since clinical efficacy and the response rate increased from 6 to 12 months of DBS treatment (Huys, et al., 2019). Further studies with a homogeneous period of stimulation and, if tolerable by the patients, longer stimulation interruption are desirable and might increase the effect of cessation of stimulation.

Seventh, because of the potential clinical significance, the validity and reliability of the correlational analyses need to be interpreted with great caution. The already mentioned restrictions of the studies, also apply here. Critically, these limitations can lead to an overestimation of the underlying interrelation between two variables. We aimed to mitigate this effect by applying Spearman rank (i.e. non-parametric) correlation analyses. Still, our findings might not translate to a broader population of OCD patients. Therefore, we advise cautious interpretation and further replication of our results. Nonetheless, the clinical interrelations might provide meaningful insights for future studies.

Finally, OCD is generally associated with hyperactivity within the cortico-striatal-thalamic loops leading to impairments in cognitive control (see section 1.1). Considering this limitation, our results must be treated with caution regarding the generalization of ALIC/NAc function in a healthy population. For obvious reasons, it is impossible to acquire LFP and DBS stimulation data in healthy participants. Therefore, we have to rely on the insights gained from

this clinical population. Merely the pre-surgery session of the **Stimulation-study** could have been compared to healthy participants, but this was outside the scope of this study. Also, results would have been of very limited value regarding the small sample size for between-group comparisons. Studies utilizing the record of long-term LFPs might help to resolve the question of LFPs alterations due to clinical change by investigating throughout the course of (successful) treatment, as has been done in the STN (Rappel, et al., 2018).

4.7. Conclusion and future directions

Despite its pivotal role in OCD symptomatology, performance monitoring processes and their relationship with clinical efficacy have yet received relatively little attention regarding ALIC/NAc DBS. Nevertheless, the correlates of error processing might turn out to be valuable biomarkers for symptom severity or DBS-induced symptom reduction in OCD. Although this interrelation should be viewed as preliminary, biomarkers with diagnostic and/or prognostic value would be of high clinical relevance. First, the a priori identification of patients that will likely benefit from an invasive and costly treatment such as DBS would be of tremendous importance. Especially, since the only efficacy predictors that have been proposed, i.e. older age at OCD onset and the presence of sexual/religious obsessions and compulsions are not yet validated. Second, intracranial biomarkers are needed for clinical applications in the context of closed-loop stimulation (Lo & Widge, 2017), whereby striatal (Widge, et al., 2019) and STN- (Rappel, et al., 2018) theta-signals for closed-loop DBS have been recently proposed. Nevertheless, the discovery of a biomarker for such a heterogenous disorder as OCD remains challenging and possibly information from various clinical characteristics, structural and electrophysiological markers will need to be combined.

So far, only a small number of studies were dedicated to the analyses of ALIC/NAc LFPs during decision conflict and error processing. Thus, the results presented here should be replicated and extended by further investigations, preferably with larger sample sizes. Also, the utilization of different cognitive control tasks (e.g. including evidence accumulation and decision under ambiguity) could be helpful to further clarify the functional significance of the ALIC/NAc in OCD. Furthermore, additional insights into performance monitoring processes and their modulation in OCD can be gained by the analyses of activity in other frequency bands, e.g. delta (1- 4 Hz; (Smith, Schuller, Huys, Baldermann, Andrade, et al., 2020)) and alpha (9-14 Hz; (Horschig, et al., 2015)) or additional analyses approaches such as phase-amplitude coupling (e.g. Cohen, et al., 2009a). Finally, further studies involving long-term acquisition of

LFPs would be particularly useful in order to confirm and extend our results regarding the clinical utility of ALIC/NAc. Overall, the results of this dissertation provide new insights in the electrophysiological correlates of the frontostriatal performance monitoring system during decision conflict and error processing as well as their modulation by clinically effective ALIC/NAc DBS. Therefore, we hope to have made a humble extension of knowledge that will facilitate the treatment in OCD.

5. References

Ahmari, S. E., Spellman, T., Douglass, N. L., Kheirbek, M. A., Simpson, H. B., Deisseroth, K., Gordon, J. A., & Hen, R. (2013). Repeated cortico-striatal stimulation generates persistent OCD-like behavior. *Science, 340*, 1234-1239.

Allen, D. P., Stegemoller, E. L., Zadikoff, C., Rosenow, J. M., & Mackinnon, C. D. (2010). Suppression of deep brain stimulation artifacts from the electroencephalogram by frequency-domain Hampel filtering. *Clin Neurophysiol, 121*, 1227-1232.

Alonso, P., Cuadras, D., Gabriels, L., Denys, D., Goodman, W., Greenberg, B. D., Jimenez-Ponce, F., Kuhn, J., Lenartz, D., Mallet, L., Nuttin, B., Real, E., Segalas, C., Schuurman, R., du Montcel, S. T., & Menchon, J. M. (2015). Deep Brain Stimulation for Obsessive-Compulsive Disorder: A Meta-Analysis of Treatment Outcome and Predictors of Response. *PLoS One, 10*, e0133591.

Avants, B., Tustison, N., & Song, G. (2008). Advanced normalization tools (ANTS). *Insight J, 1–35*.

Avants, B. B., Epstein, C. L., Grossman, M., & Gee, J. C. (2008). Symmetric diffeomorphic image registration with cross-correlation: evaluating automated labeling of elderly and neurodegenerative brain. *Med Image Anal, 12*, 26-41.

Baldermann, J. C., Melzer, C., Zapf, A., Kohl, S., Timmermann, L., Tittgemeyer, M., Huys, D., Visser-Vandewalle, V., Kuhn, A. A., Horn, A., & Kuhn, J. (2019). Connectivity Profile Predictive of Effective Deep Brain Stimulation in Obsessive-Compulsive Disorder. *Biol Psychiatry, 85*, 735-743.

Baniasadi, M., Proverbio, D., Goncalves, J., Hertel, F., & Husch, A. (2020). FastField: An open-source toolbox for efficient approximation of deep brain stimulation electric fields. *Neuroimage, 223*, 117330.

Bartholow, B. D., Pearson, M. A., Dickter, C. L., Sher, K. J., Fabiani, M., & Gratton, G. (2005). Strategic control and medial frontal negativity: beyond errors and response conflict. *Psychophysiology, 42*, 33-42.

Benabid, A. L., Pollak, P., Louveau, A., Henry, S., & de Rougemont, J. (1987). Combined (thalamotomy and stimulation) stereotactic surgery of the VIM thalamic nucleus for bilateral Parkinson disease. *Appl Neurophysiol, 50*, 344-346.

Benjamini, Y., & Hochberg, Y. (1995). Controlling the False Discovery Rate - a Practical and Powerful Approach to Multiple Testing. *Journal of the Royal Statistical Society Series B-Statistical Methodology, 57*, 289-300.

Beucke, J. C., Sepulcre, J., Talukdar, T., Linnman, C., Zschenderlein, K., Endrass, T., Kaufmann, C., & Kathmann, N. (2013). Abnormally high degree connectivity of the orbitofrontal cortex in obsessive-compulsive disorder. *JAMA Psychiatry, 70*, 619-629.

Botvinick, M. M., Braver, T. S., Barch, D. M., Carter, C. S., & Cohen, J. D. (2001). Conflict monitoring and cognitive control. *Psychol Rev, 108*, 624-652.

Brady, A. M., & O'Donnell, P. (2004). Dopaminergic modulation of prefrontal cortical input to nucleus accumbens neurons in vivo. *J Neurosci, 24*, 1040-1049.

Brown, P., & Williams, D. (2005). Basal ganglia local field potential activity: character and functional significance in the human. *Clin Neurophysiol, 116*, 2510-2519.

Burguiere, E., Monteiro, P., Mallet, L., Feng, G., & Graybiel, A. M. (2015). Striatal circuits, habits, and implications for obsessive-compulsive disorder. *Curr Opin Neurobiol, 30*, 59-65.

Buzsáki, G., Anastassiou, C. A., & Koch, C. (2012). The origin of extracellular fields and currents—EEG, ECoG, LFP and spikes. *Nature reviews neuroscience, 13*, 407-420.

Carrasco, M., Harbin, S. M., Nienhuis, J. K., Fitzgerald, K. D., Gehring, W. J., & Hanna, G. L. (2013). Increased error-related brain activity in youth with obsessive-compulsive disorder and unaffected siblings. *Depression and Anxiety, 30*, 39-46.

Cavanagh, J. F., Cohen, M. X., & Allen, J. J. (2009). Prelude to and resolution of an error: EEG phase synchrony reveals cognitive control dynamics during action monitoring. *J Neurosci, 29*, 98-105.

Cavanagh, J. F., & Frank, M. J. (2014). Frontal theta as a mechanism for cognitive control. *Trends Cogn Sci, 18*, 414-421.

Cavanagh, J. F., Wiecki, T. V., Cohen, M. X., Figueroa, C. M., Samanta, J., Sherman, S. J., & Frank, M. J. (2011). Subthalamic nucleus stimulation reverses mediofrontal influence over decision threshold. *Nat Neurosci, 14*, 1462-1467.

Cavanagh, J. F., Zambrano-Vazquez, L., & Allen, J. J. (2012). Theta lingua franca: a common mid-frontal substrate for action monitoring processes. *Psychophysiology, 49*, 220-238.

Cohen, M. X. (2011). Error-related medial frontal theta activity predicts cingulate-related structural connectivity. *Neuroimage, 55*, 1373-1383.

Cohen, M. X. (2014). *Analyzing neural time series data: theory and practice*: MIT Press.

Cohen, M. X., Axmacher, N., Lenartz, D., Elger, C. E., Sturm, V., & Schlaepfer, T. E. (2009a). Good vibrations: cross-frequency coupling in the human nucleus accumbens during reward processing. *J Cogn Neurosci, 21*, 875-889.

Cohen, M. X., Axmacher, N., Lenartz, D., Elger, C. E., Sturm, V., & Schlaepfer, T. E. (2009b). Neuroelectric signatures of reward learning and decision-making in the human nucleus accumbens. *Neuropsychopharmacology, 34*, 1649-1658.

Cohen, M. X., Axmacher, N., Lenartz, D., Elger, C. E., Sturm, V., & Schlaepfer, T. E. (2009c). Nuclei accumbens phase synchrony predicts decision-making reversals following negative feedback. *J Neurosci, 29*, 7591-7598.

Cohen, M. X., Bour, L., Mantione, M., Figee, M., Vink, M., Tijssen, M. A., van Rootselaar, A. F., van den Munckhof, P., Schuurman, P. R., & Denys, D. (2012). Top-down-directed synchrony from medial frontal cortex to nucleus accumbens during reward anticipation. *Hum Brain Mapp, 33*, 246-252.

Cohen, M. X., & Cavanagh, J. F. (2011). Single-trial regression elucidates the role of prefrontal theta oscillations in response conflict. *Front Psychol, 2*, 30.

Cohen, M. X., Elger, C. E., & Ranganath, C. (2007). Reward expectation modulates feedback-related negativity and EEG spectra. *Neuroimage, 35*, 968-978.

Cohen, M. X., Ridderinkhof, K. R., Haupt, S., Elger, C. E., & Fell, J. (2008). Medial frontal cortex and response conflict: evidence from human intracranial EEG and medial frontal cortex lesion. *Brain Res, 1238*, 127-142.

Coles, M. G. H., Scheffers, M. K., & Holroyd, C. B. (2001). Why is there an ERN/Ne on correct trials? Response representations, stimulus-related components, and the theory of error-processing. *Biological psychology, 56*, 173-189.

Danielmeier, C., Wessel, J. R., Steinhauser, M., & Ullsperger, M. (2009). Modulation of the error-related negativity by response conflict. *Psychophysiology, 46*, 1288-1298.

de Bruijn, E. R., Hulstijn, W., Verkes, R. J., Ruigt, G. S., & Sabbe, B. G. (2004). Drug-induced stimulation and suppression of action monitoring in healthy volunteers. *Psychopharmacology (Berl), 177*, 151-160.

Delorme, A., & Makeig, S. (2004). EEGLAB: an open source toolbox for analysis of single-trial EEG dynamics including independent component analysis. *J Neurosci Methods, 134*, 9-21.

Dembek, T. A., Barbe, M. T., Astrom, M., Hoevels, M., Visser-Vandewalle, V., Fink, G. R., & Timmermann, L. (2017). Probabilistic mapping of deep brain stimulation effects in essential tremor. *Neuroimage Clin, 13*, 164-173.

Denys, D., Graat, I., Mocking, R., de Koning, P., Vulink, N., Figee, M., Ooms, P., Mantione, M., van den Munckhof, P., & Schuurman, R. (2020). Efficacy of Deep Brain Stimulation of the Ventral Anterior Limb of the Internal Capsule for Refractory Obsessive-Compulsive Disorder: A Clinical Cohort of 70 Patients. *Am J Psychiatry, 177*, 265-271.

Denys, D., Mantione, M., Figee, M., van den Munckhof, P., Koerselman, F., Westenberg, H., Bosch, A., & Schuurman, R. (2010). Deep brain stimulation of the nucleus accumbens for treatment-refractory obsessive-compulsive disorder. *Arch Gen Psychiatry, 67*, 1061-1068.

Eddy, K. T., Dutra, L., Bradley, R., & Westen, D. (2004). A multidimensional meta-analysis of psychotherapy and pharmacotherapy for obsessive-compulsive disorder. *Clin Psychol Rev, 24*, 1011-1030.

Eijsker, N., van Wingen, G., Smolders, R., Smit, D. J. A., & Denys, D. (2020). Exploring the Role of the Nucleus Accumbens in Adaptive Behavior Using Concurrent Intracranial and Extracranial Electrophysiological Recordings in Humans. *eNeuro, 7*.

Endrass, T., Klawohn, J., Schuster, F., & Kathmann, N. (2008). Overactive performance monitoring in obsessive-compulsive disorder: ERP evidence from correct and erroneous reactions. *Neuropsychologia, 46*, 1877-1887.

Endrass, T., Schuermann, B., Kaufmann, C., Spielberg, R., Kniesche, R., & Kathmann, N. (2010). Performance monitoring and error significance in patients with obsessive-compulsive disorder. *Biol Psychol, 84*, 257-263.

Endrass, T., & Ullsperger, M. (2014). Specificity of performance monitoring changes in obsessive-compulsive disorder. *Neurosci Biobehav Rev, 46 Pt 1*, 124-138.

Eriksen, B. A., & Eriksen, C. W. (1974). Effects of noise letters upon the identification of a target letter in a nonsearch task. *Perception & Psychophysics, 16*, 143-149.

Falkenstein, M., Hohnsbein, J., Hoormann, J., & Blanke, L. (1990). Effects of errors in choice reaction tasks on the ERP under focused and divided attention. *Psychophysiological brain research, 1*, 192-195.

Falkenstein, M., Hohnsbein, J., Hoormann, J., & Blanke, L. (1991). Effects of crossmodal divided attention on late ERP components. II. Error processing in choice reaction tasks. *Electroencephalogr Clin Neurophysiol, 78*, 447-455.

Falkenstein, M., Hoormann, J., Christ, S., & Hohnsbein, J. (2000). ERP components on reaction errors and their functional significance: a tutorial. *Biological psychology, 51*, 87-107.

Figee, M., Luigjes, J., Smolders, R., Valencia-Alfonso, C. E., van Wingen, G., de Kwaasteniet, B., Mantione, M., Ooms, P., de Koning, P., Vulink, N., Levar, N., Droge, L., van den Munckhof, P., Schuurman, P. R., Nederveen, A., van den Brink, W., Mazaheri, A., Vink, M., & Denys, D. (2013). Deep brain stimulation restores frontostriatal network activity in obsessive-compulsive disorder. *Nat Neurosci, 16*, 386-387.

Fischer, A. G., Klein, T. A., & Ullsperger, M. (2017). Comparing the error-related negativity across groups: The impact of error- and trial-number differences. *Psychophysiology, 54*, 998-1009.

Fitzgerald, K. D., Welsh, R. C., Gehring, W. J., Abelson, J. L., Himle, J. A., Liberzon, I., & Taylor, S. F. (2005). Error-related hyperactivity of the anterior cingulate cortex in obsessive-compulsive disorder. *Biol Psychiatry, 57*, 287-294.

Fonov, V., Evans, A. C., Botteron, K., Almli, C. R., McKinstry, R. C., Collins, D. L., & Brain Development Cooperative, G. (2011). Unbiased average age-appropriate atlases for pediatric studies. *Neuroimage, 54*, 313-327.

Frank, M. J. (2006). Hold your horses: a dynamic computational role for the subthalamic nucleus in decision making. *Neural Netw, 19*, 1120-1136.

Frank, M. J., Loughry, B., & O'Reilly, R. C. (2001). Interactions between frontal cortex and basal ganglia in working memory: a computational model. *Cogn Affect Behav Neurosci, 1*, 137-160.

Gehring, W. J., Goss, B., Coles, M. G. H., Meyer, D. E., & Donchin, E. (2016). A Neural System for Error Detection and Compensation. *Psychological Science, 4*, 385-390.

Gehring, W. J., Himle, J., & Nisenson, L. G. (2000). Action-monitoring dysfunction in obsessive-compulsive disorder. *Psychological Science, 11*, 1-6.

Goodman, W. K., Foote, K. D., Greenberg, B. D., Ricciuti, N., Bauer, R., Ward, H., Shapira, N. A., Wu, S. S., Hill, C. L., Rasmussen, S. A., & Okun, M. S. (2010). Deep brain stimulation for intractable obsessive compulsive disorder: pilot study using a blinded, staggered-onset design. *Biol Psychiatry, 67*, 535-542.

Goodman, W. K., Price, L. H., Rasmussen, S. A., Mazure, C., Fleischmann, R. L., Hill, C. L., Heninger, G. R., & Charney, D. S. (1989). The Yale-Brown Obsessive Compulsive Scale. I. Development, use, and reliability. *Arch Gen Psychiatry, 46*, 1006-1011.

Goto, Y., & Grace, A. A. (2005). Dopaminergic modulation of limbic and cortical drive of nucleus accumbens in goal-directed behavior. *Nat Neurosci, 8*, 805-812.

Grace, A. A., Floresco, S. B., Goto, Y., & Lodge, D. J. (2007). Regulation of firing of dopaminergic neurons and control of goal-directed behaviors. *Trends Neurosci, 30*, 220-227.

Grados, M., & Riddle, M. A. (2008). Do all obsessive-compulsive disorder subtypes respond to medication? *Int Rev Psychiatry, 20*, 189-193.

Greenberg, B. D., Gabriels, L. A., Malone, D. A., Jr., Rezai, A. R., Friehs, G. M., Okun, M. S., Shapira, N. A., Foote, K. D., Cosyns, P. R., Kubu, C. S., Malloy, P. F., Salloway, S. P., Giftakis, J. E., Rise, M. T., Machado, A. G., Baker, K. B., Stypulkowski, P. H., Goodman, W. K., Rasmussen, S. A., & Nuttin, B. J. (2010). Deep brain stimulation of the ventral internal capsule/ventral striatum for obsessive-compulsive disorder: worldwide experience. *Mol Psychiatry, 15*, 64-79.

Grundler, T. O., Cavanagh, J. F., Figueroa, C. M., Frank, M. J., & Allen, J. J. (2009). Task-related dissociation in ERN amplitude as a function of obsessive-compulsive symptoms. *Neuropsychologia, 47*, 1978-1987.

Gu, B. M., Park, J. Y., Kang, D. H., Lee, S. J., Yoo, S. Y., Jo, H. J., Choi, C. H., Lee, J. M., & Kwon, J. S. (2008). Neural correlates of cognitive inflexibility during task-switching in obsessive-compulsive disorder. *Brain, 131*, 155-164.

Haber, S. N., Fudge, J. L., & McFarland, N. R. (2000). Striatonigrostriatal pathways in primates form an ascending spiral from the shell to the dorsolateral striatum. *J Neurosci, 20*, 2369-2382.

Haber, S. N., & Knutson, B. (2010). The reward circuit: linking primate anatomy and human imaging. *Neuropsychopharmacology, 35*, 4-26.

Haber, S. N., Kunishio, K., Mizobuchi, M., & Lyndbalta, E. (1995). The Orbital and Medial Prefrontal Circuit through the Primate Basal Ganglia. *Journal of Neuroscience, 15*, 4851-4867.

Haber, S. N., Yendiki, A., & Jbabdi, S. (2020). Four Deep Brain Stimulation Targets for Obsessive-Compulsive Disorder: Are They Different? *Biol Psychiatry*.

Hajcak, G., Franklin, M. E., Foa, E. B., & Simons, R. F. (2008). Increased error-related brain activity in pediatric obsessive-compulsive disorder before and after treatment. *Am J Psychiatry, 165*, 116-123.

Handy, T. C. (2005). *Event-related potentials: A methods handbook*: MIT press.

Harrison, B. J., Soriano-Mas, C., Pujol, J., Ortiz, H., Lopez-Sola, M., Hernandez-Ribas, R., Deus, J., Alonso, P., Yucel, M., Pantelis, C., Menchon, J. M., & Cardoner, N. (2009). Altered corticostriatal functional connectivity in obsessive-compulsive disorder. *Arch Gen Psychiatry, 66*, 1189-1200.

Heinze, H. J., Heldmann, M., Voges, J., Hinrichs, H., Marco-Pallares, J., Hopf, J. M., Muller, U. J., Galazky, I., Sturm, V., Bogerts, B., & Munte, T. F. (2009). Counteracting incentive sensitization in severe alcohol dependence using deep brain stimulation of the nucleus accumbens: clinical and basic science aspects. *Front Hum Neurosci, 3*, 22.

Holroyd, C. B., & Coles, M. G. H. (2002). The neural basis of human error processing: reinforcement learning, dopamine, and the error-related negativity. *Psychol Rev, 109*, 679-709.

Holtzheimer, P. E., & Mayberg, H. S. (2011). Deep brain stimulation for psychiatric disorders. *Annu Rev Neurosci, 34*, 289-307.

Horn, A., & Kuhn, A. A. (2015). Lead-DBS: a toolbox for deep brain stimulation electrode localizations and visualizations. *Neuroimage, 107*, 127-135.

Horn, A., Li, N., Dembek, T. A., Kappel, A., Boulay, C., Ewert, S., Tietze, A., Husch, A., Perera, T., Neumann, W. J., Reisert, M., Si, H., Oostenveld, R., Rorden, C., Yeh, F. C., Fang, Q., Herrington, T. M., Vorwerk, J., & Kuhn, A. A. (2019). Lead-DBS v2: Towards a comprehensive pipeline for deep brain stimulation imaging. *Neuroimage, 184*, 293-316.

Horschig, J. M., Smolders, R., Bonnefond, M., Schoffelen, J. M., van den Munckhof, P., Schuurman, P. R., Cools, R., Denys, D., & Jensen, O. (2015). Directed Communication between Nucleus Accumbens and Neocortex in Humans Is Differentially Supported by Synchronization in the Theta and Alpha Band. *PLoS One, 10*, e0138685.

Husch, A., M, V. P., Gemmar, P., Goncalves, J., & Hertel, F. (2018). PaCER - A fully automated method for electrode trajectory and contact reconstruction in deep brain stimulation. *Neuroimage Clin, 17*, 80-89.

Huys, D., Kohl, S., Baldermann, J. C., Timmermann, L., Sturm, V., Visser-Vandewalle, V., & Kuhn, J. (2019). Open-label trial of anterior limb of internal capsule-nucleus accumbens deep brain stimulation for obsessive-compulsive disorder: insights gained. *J Neurol Neurosurg Psychiatry, 90*, 805-812.

Jackson, M. E., Frost, A. S., & Moghaddam, B. (2001). Stimulation of prefrontal cortex at physiologically relevant frequencies inhibits dopamine release in the nucleus accumbens. *Journal of Neurochemistry, 78*, 920-923.

Jasper, H. H. (1958). Report of the committee on methods of clinical examination in electroencephalography. *Electroencephalography and Clinical Neurophysiology, 10*, 370-375.

Kaczkurkin, A. N. (2013). The effect of manipulating task difficulty on error-related negativity in individuals with obsessive-compulsive symptoms. *Biol Psychol, 93*, 122-131.

Kohl, S., Schonherr, D. M., Luigjes, J., Denys, D., Mueller, U. J., Lenartz, D., Visser-Vandewalle, V., & Kuhn, J. (2014). Deep brain stimulation for treatment-refractory obsessive compulsive disorder: a systematic review. *BMC Psychiatry, 14*, 214.

Kopp, B., Rist, F., & Mattler, U. (1996). N200 in the flanker task as a neurobehavioral tool for investigating executive control. *Psychophysiology, 33*, 282-294.

Koran, L. M., Hanna, G. L., Hollander, E., Nestadt, G., Simpson, H. B., & American Psychiatric, A. (2007). Practice guideline for the treatment of patients with obsessive-compulsive disorder. *Am J Psychiatry, 164*, 5-53.

Krack, P., Volkmann, J., Tinkhauser, G., & Deuschl, G. (2019). Deep Brain Stimulation in Movement Disorders: From Experimental Surgery to Evidence-Based Therapy. *Mov Disord, 34*, 1795-1810.

Kuhn, J., Grundler, T. O., Bauer, R., Huff, W., Fischer, A. G., Lenartz, D., Maarouf, M., Buhrle, C., Klosterkotter, J., Ullsperger, M., & Sturm, V. (2011). Successful deep brain stimulation of the nucleus accumbens in severe alcohol dependence is associated with changed performance monitoring. *Addict Biol, 16*, 620-623.

Kuhn, J., Grundler, T. O., Lenartz, D., Sturm, V., Klosterkotter, J., & Huff, W. (2010). Deep brain stimulation for psychiatric disorders. *Dtsch Arztebl Int, 107*, 105-113.

Lempka, S. F., & McIntyre, C. C. (2013). Theoretical analysis of the local field potential in deep brain stimulation applications. *PLoS One, 8*, e59839.

Li, N., Baldermann, J. C., Kibleur, A., Treu, S., Akram, H., Elias, G. J. B., Boutet, A., Lozano, A. M., Al-Fatly, B., Strange, B., Barcia, J. A., Zrinzo, L., Joyce, E., Chabardes, S., Visser-Vandewalle, V., Polosan, M., Kuhn, J., Kuhn, A. A., & Horn, A. (2020). A unified connectomic target for deep brain stimulation in obsessive-compulsive disorder. *Nat Commun, 11*, 3364.

Lo, M. C., & Widge, A. S. (2017). Closed-loop neuromodulation systems: next-generation treatments for psychiatric illness. *Int Rev Psychiatry, 29*, 191-204.

Luck, S. J. (2005). *An introduction to the event related potential technique*: MIT Press.

Luu, P., & Tucker, D. M. (2001). Regulating action: alternating activation of midline frontal and motor cortical networks. *Clin Neurophysiol, 112*, 1295-1306.

Luu, P., Tucker, D. M., & Makeig, S. (2004). Frontal midline theta and the error-related negativity: neurophysiological mechanisms of action regulation. *Clin Neurophysiol, 115*, 1821-1835.

Makeig, S., Debener, S., Onton, J., & Delorme, A. (2004). Mining event-related brain dynamics. *Trends Cogn Sci, 8*, 204-210.

Mandali, A., Weidacker, K., Kim, S. G., & Voon, V. (2019). The ease and sureness of a decision: evidence accumulation of conflict and uncertainty. *Brain, 142*, 1471-1482.

Marmor, O., Valsky, D., Joshua, M., Bick, A. S., Arkadir, D., Tamir, I., Bergman, H., Israel, Z., & Eitan, R. (2017). Local vs. volume conductance activity of field potentials in the human subthalamic nucleus. *J Neurophysiol, 117*, 2140-2151.

McIntyre, C. C., & Hahn, P. J. (2010). Network perspectives on the mechanisms of deep brain stimulation. *Neurobiology of Disease, 38*, 329-337.

Melcher, T., Falkai, P., & Gruber, O. (2008). Functional brain abnormalities in psychiatric disorders: neural mechanisms to detect and resolve cognitive conflict and interference. *Brain Res Rev, 59*, 96-124.

Milad, M. R., & Rauch, S. L. (2012). Obsessive-compulsive disorder: beyond segregated cortico-striatal pathways. *Trends Cogn Sci, 16*, 43-51.

Mithani, K., Davison, B., Meng, Y., & Lipsman, N. (2020). The anterior limb of the internal capsule: Anatomy, function, and dysfunction. *Behav Brain Res, 387*, 112588.

Mogenson, G. J., Jones, D. L., & Yim, C. Y. (1980). From Motivation to Action - Functional Interface between the Limbic System and the Motor System. *Progress in Neurobiology, 14*, 69-97.

Munte, T. F., Heldmann, M., Hinrichs, H., Marco-Pallares, J., Kramer, U. M., Sturm, V., & Heinze, H. J. (2007). Nucleus Accumbens is Involved in Human Action Monitoring: Evidence from Invasive Electrophysiological Recordings. *Front Hum Neurosci, 1*, 11.

Munte, T. F., Heldmann, M., Hinrichs, H., Marco-Pallares, J., Kramer, U. M., Sturm, V., & Heinze, H. J. (2008). Contribution of subcortical structures to cognition assessed with invasive electrophysiology in humans. *Front Neurosci, 2*, 72-78.

Murray, C. J., & Lopez, A. D. (1996). Evidence-based health policy--lessons from the Global Burden of Disease Study. *Science, 274*, 740-743.

Nuttin, B., Cosyns, P., Demeulemeester, H., Gybels, J., & Meyerson, B. (1999). Electrical stimulation in anterior limbs of internal capsules in patients with obsessive-compulsive disorder. *Lancet, 354*, 1526.

Pauli, W. M., Nili, A. N., & Tyszka, J. M. (2017). A High-Resolution Probabilistic In Vivo Atlas of Human Subcortical Brain Nuclei. *bioRxiv*.

Pauls, D. L., Abramovitch, A., Rauch, S. L., & Geller, D. A. (2014). Obsessive-compulsive disorder: an integrative genetic and neurobiological perspective. *Nat Rev Neurosci, 15*, 410-424.

Perera, M. P. N., Bailey, N. W., Herring, S. E., & Fitzgerald, P. B. (2019). Electrophysiology of obsessive compulsive disorder: A systematic review of the electroencephalographic literature. *J Anxiety Disord, 62*, 1-14.

Rappel, P., Marmor, O., Bick, A. S., Arkadir, D., Linetsky, E., Castrioto, A., Tamir, I., Freedman, S. A., Mevorach, T., Gilad, M., Bergman, H., Israel, Z., & Eitan, R. (2018). Subthalamic theta activity: a novel human subcortical biomarker for obsessive compulsive disorder. *Transl Psychiatry, 8*, 118.

Riesel, A. (2019). The erring brain: Error-related negativity as an endophenotype for OCD-A review and meta-analysis. *Psychophysiology, 56*, e13348.

Riesel, A., Endrass, T., Auerbach, L. A., & Kathmann, N. (2015). Overactive Performance Monitoring as an Endophenotype for Obsessive-Compulsive Disorder: Evidence From a Treatment Study. *Am J Psychiatry, 172*, 665-673.

Riesel, A., Endrass, T., Kaufmann, C., & Kathmann, N. (2011). Overactive error-related brain activity as a candidate endophenotype for obsessive-compulsive disorder: evidence from unaffected first-degree relatives. *Am J Psychiatry, 168*, 317-324.

Riesel, A., Kathmann, N., & Endrass, T. (2014). Overactive performance monitoring in obsessive-compulsive disorder is independent of symptom expression. *Eur Arch Psychiatry Clin Neurosci, 264*, 707-717.

Riesel, A., Klawohn, J., Kathmann, N., & Endrass, T. (2017). Conflict monitoring and adaptation as reflected by N2 amplitude in obsessive-compulsive disorder. *Psychol Med, 47*, 1379-1388.

Salgado, S., & Kaplitt, M. G. (2015). The Nucleus Accumbens: A Comprehensive Review. *Stereotact Funct Neurosurg, 93*, 75-93.

Schonecker, T., Kupsch, A., Kuhn, A. A., Schneider, G. H., & Hoffmann, K. T. (2009). Automated optimization of subcortical cerebral MR imaging-atlas coregistration for improved postoperative electrode localization in deep brain stimulation. *AJNR Am J Neuroradiol, 30*, 1914-1921.

Schuller, T., Gruendler, T. O., Jocham, G., Klein, T. A., Timmermann, L., Visser-Vandewalle, V., Kuhn, J., & Ullsperger, M. (2015). Rapid feedback processing in human nucleus accumbens and motor thalamus. *Neuropsychologia, 70*, 246-254.

Seifert, J. (2005). *Ereigniskorrelierte EEG-Aktivität*: Pabst Lengerich, Germany.

Shephard, E., Stern, E. R., van den Heuvel, O. A., Costa, D. L. C., Batistuzzo, M. C., Godoy, P. B. G., Lopes, A. C., Brunoni, A. R., Hoexter, M. Q., Shavitt, R. G., Reddy, Y. C. J., Lochner, C., Stein, D. J., Simpson, H. B., & Miguel, E. C. (2021). Toward a neurocircuit-based taxonomy to guide treatment of obsessive-compulsive disorder. *Mol Psychiatry*.

Siegert, S., Herrojo Ruiz, M., Brucke, C., Huebl, J., Schneider, G. H., Ullsperger, M., & Kuhn, A. A. (2014). Error signals in the subthalamic nucleus are related to post-error slowing in patients with Parkinson's disease. *Cortex, 60*, 103-120.

Sildatke, E., Gruendler, T. O. J., Ullsperger, M., Dembek, T. A., Baldermann, J. C., Kohl, S., Visser-Vandewalle, V., Huys, D., Kuhn, J., & Schuller, T. (2021). Deep Brain Stimulation Reduces Conflict-Related Theta and Error-Related Negativity in Patients With Obsessive-Compulsive Disorder. *Neuromodulation*.

Sildatke, E., & Schüller, T. (in preparation). Conflict- and Error-Related Theta in the ALIC/NAc of Patients with Obsessive-Compulsive Disorder.

Sildatke, E., Schuller, T., Grundler, T. O. J., Ullsperger, M., Visser-Vandewalle, V., Huys, D., & Kuhn, J. (2020). Error-Related Activity in Striatal Local Field Potentials and Medial Frontal Cortex: Evidence From Patients With Severe Opioid Abuse Disorder. *Front Hum Neurosci, 14*, 627564.

Smith, E. E., Schuller, T., Huys, D., Baldermann, J. C., Andrade, P., Allen, J. J., Visser-Vandewalle, V., Ullsperger, M., Gruendler, T. O. J., & Kuhn, J. (2020). A brief demonstration of frontostriatal connectivity in OCD patients with intracranial electrodes. *Neuroimage, 220*, 117138.

Smith, E. E., Schuller, T., Huys, D., Baldermann, J. C., Ullsperger, M., Allen, J. J., Visser-Vandewalle, V., Kuhn, J., & Gruendler, T. O. J. (2020). Prefrontal delta oscillations during deep brain stimulation predict treatment success in patients with obsessive-compulsive disorder. *Brain Stimul, 13*, 259-261.

Smolders, R., Mazaheri, A., van Wingen, G., Figee, M., de Koning, P. P., & Denys, D. (2013). Deep brain stimulation targeted at the nucleus accumbens decreases the potential for pathologic network communication. *Biol Psychiatry, 74*, e27-28.

Stern, E. R., Liu, Y., Gehring, W. J., Lister, J. J., Yin, G., Zhang, J., Fitzgerald, K. D., Himle, J. A., Abelson, J. L., & Taylor, S. F. (2010). Chronic medication does not affect hyperactive error responses in obsessive-compulsive disorder. *Psychophysiology, 47*, 913-920.

Trujillo, L. T., & Allen, J. J. (2007). Theta EEG dynamics of the error-related negativity. *Clin Neurophysiol, 118*, 645-668.

Ullsperger, M., Danielmeier, C., & Jocham, G. (2014). Neurophysiology of performance monitoring and adaptive behavior. *Physiol Rev, 94*, 35-79.

Ullsperger, M., Fischer, A. G., Nigbur, R., & Endrass, T. (2014). Neural mechanisms and temporal dynamics of performance monitoring. *Trends Cogn Sci, 18*, 259-267.

Ullsperger, M., & von Cramon, D. Y. (2006). The role of intact frontostriatal circuits in error processing. *J Cogn Neurosci, 18*, 651-664.

van den Heuvel, O. A., van Wingen, G., Soriano-Mas, C., Alonso, P., Chamberlain, S. R., Nakamae, T., Denys, D., Goudriaan, A. E., & Veltman, D. J. (2016). Brain circuitry of compulsivity. *Eur Neuropsychopharmacol, 26*, 810-827.

van Westen, M., Rietveld, E., Figee, M., & Denys, D. (2015). Clinical Outcome and Mechanisms of Deep Brain Stimulation for Obsessive-Compulsive Disorder. *Curr Behav Neurosci Rep, 2*, 41-48.

Veerakumar, A., & Berton, O. (2015). Cellular mechanisms of deep brain stimulation: activity-dependent focal circuit reprogramming? *Curr Opin Behav Sci, 4*, 48-55.

Vinck, M., Oostenveld, R., van Wingerden, M., Battaglia, F., & Pennartz, C. M. (2011). An improved index of phase-synchronization for electrophysiological data in the presence of volume-conduction, noise and sample-size bias. *Neuroimage, 55*, 1548-1565.

Voges, J., Muller, U., Bogerts, B., Munte, T., & Heinze, H. J. (2013). Deep brain stimulation surgery for alcohol addiction. *World Neurosurg, 80*, S28 e21-31.

Widge, A. S., Zorowitz, S., Basu, I., Paulk, A. C., Cash, S. S., Eskandar, E. N., Deckersbach, T., Miller, E. K., & Dougherty, D. D. (2019). Deep brain stimulation of the internal capsule enhances human cognitive control and prefrontal cortex function. *Nat Commun, 10*, 1536.

Wiecki, T. V., & Frank, M. J. (2013). A computational model of inhibitory control in frontal cortex and basal ganglia. *Psychol Rev, 120*, 329-355.

Winter, L., Alam, M., Heissler, H. E., Saryyeva, A., Milakara, D., Jin, X., Heitland, I., Schwabe, K., Krauss, J. K., & Kahl, K. G. (2019). Neurobiological Mechanisms of Metacognitive Therapy – An Experimental Paradigm. *Frontiers in psychology, 10*, 660.

Wittchen, H. U., Jacobi, F., Rehm, J., Gustavsson, A., Svensson, M., Jonsson, B., Olesen, J., Allgulander, C., Alonso, J., Faravelli, C., Fratiglioni, L., Jennum, P., Lieb, R., Maercker, A., van Os, J., Preisig, M., Salvador-Carulla, L., Simon, R., & Steinhausen, H. C. (2011). The size and burden of mental disorders and other disorders of the brain in Europe 2010. *Eur Neuropsychopharmacol, 21*, 655-679.

Yeung, N., Botvinick, M. M., & Cohen, J. D. (2004). The neural basis of error detection: conflict monitoring and the error-related negativity. *Psychol Rev, 111*, 931-959.

Zavala, B., Brittain, J. S., Jenkinson, N., Ashkan, K., Foltynie, T., Limousin, P., Zrinzo, L., Green, A. L., Aziz, T., Zaghloul, K., & Brown, P. (2013). Subthalamic nucleus local field potential activity during the Eriksen flanker task reveals a novel role for theta phase during conflict monitoring. *J Neurosci, 33*, 14758-14766.

Zavala, B., Zaghloul, K., & Brown, P. (2015). The subthalamic nucleus, oscillations, and conflict. *Mov Disord, 30*, 328-338.

Zavala, B. A., Tan, H., Little, S., Ashkan, K., Hariz, M., Foltynie, T., Zrinzo, L., Zaghloul, K. A., & Brown, P. (2014). Midline frontal cortex low-frequency activity drives subthalamic nucleus oscillations during conflict. *J Neurosci, 34*, 7322-7333.

6. Danksagung

Ich möchte mich an dieser Stelle bei all denjenigen bedanken ohne deren Beteiligung und/oder Unterstützung diese Dissertation nicht möglich wäre.

Zunächst möchte ich mich recht herzlich bei Prof. Dr. Jens Kuhn bedanken, der mir die Möglichkeit zu dieser Arbeit überhaupt eröffnet hat. Jens, ich danke dir sehr für das stets entgegengebrachte Vertrauern, Motivation, Wertschätzung und Unterstützung.

Des Weiteren möchte ich mich bei meinen Kollegen der Arbeitsgruppe „Neurobiologie und Neuromodulation psychiatrischer Erkrankungen“ bedanken. Ich schätze euch sehr und bin dankbar für die freudige Zusammenarbeit. Ein besonderer Dank gilt hierbei Dr. Thomas Schüller, der mir in der Welt des EEGs fortwährend den Weg wies. Thomas, ich danke dir vielmals für deine enorme Unterstützung, stetige Motivation und ausdauernde Geduld.

Ein großer Dank gilt außerdem meiner Familie und meinen Freunden für eure fortwährende Unterstützen, Verständnis und Zuversicht. Insbesondere danke ich meinen Eltern und meinen Schwiegereltern für den starken Rückhalt, vor allem in schwierigen Phasen dieser Arbeit und des gesamten Studiums.

Vom ganzen Herzen danke ich meinem Ehemann Marcel für seine bedingungslose Unterstützung. Bei jedem Weg den ich eigenschlagen habe hast du mir Mut zugesprochen, Verständnis entgegengebracht und mir den nötigen Raum zur Verwirklichung gewährt. Ich danke dir für deine liebevolle Fürsorge als Freund, Ehemann und Familienvater.

Schließlich danke ich meinem kleinen Racker, der mich immer zum Lachen bringt und mich alles Drumherum vergessen lässt. Danke, dass du meinen Blick auf das Wesentliche lenkst.

Vielen Dank!

7. Erklärung

Hiermit versichere ich an Eides statt, dass ich die vorliegende Dissertationsschrift selbstständig und ohne die Benutzung anderer als der angegebenen Hilfsmittel angefertigt habe. Alle Stellen - einschließlich Tabellen, Karten und Abbildungen -, die wörtlich oder sinngemäß aus veröffentlichten und nicht veröffentlichten anderen Werken im Wortlaut oder dem Sinn nach entnommen sind, sind in jedem Einzelfall als Entlehnung kenntlich gemacht. Ich versichere an Eides statt, dass diese Dissertationsschrift noch keiner anderen Fakultät oder Universität zur Prüfung vorgelegen hat; dass sie - abgesehen von unten angegebenen Teilpublikationen - noch nicht veröffentlicht worden ist sowie, dass ich eine solche Veröffentlichung vor Abschluss der Promotion nicht ohne Genehmigung der / des Vorsitzenden des IPHS-Promotionsausschusses vornehmen werde. Die Bestimmungen dieser Ordnung sind mir bekannt. Die von mir vorgelegte Dissertation ist von Prof. Dr. Jens Kuhn betreut worden.

Darüber hinaus erkläre ich hiermit, dass ich die Ordnung zur Sicherung guter wissenschaftlicher Praxis und zum Umgang mit wissenschaftlichem Fehlverhalten der Universität zu Köln gelesen und sie bei der Durchführung der Dissertation beachtet habe und verpflichte mich hiermit, die dort genannten Vorgaben bei allen wissenschaftlichen Tätigkeiten zu beachten und umzusetzen.

Übersicht der Publikationen:

Sildatke, E., Grundler, T.O.J., Ullsperger, M., Dembek, T.A., Baldermann, J.C., Kohl, S., Visser-Vandewalle, V., Huys, D., Kuhn, J., and Schüller, T. (2021). Deep Brain Stimulation Reduces Conflict-Related Theta and Error-Related Negativity in Patients with Obsessive-Compulsive Disorder. *Neuromodulation*.

Sildatke, E., and Schüller, T. (in preparation). Conflict- and Error-Related Theta in the ALIC/NAc of Patients with Obsessive-Compulsive Disorder.

Ich versichere, dass ich alle Angaben wahrheitsgemäß nach bestem Wissen und Gewissen gemacht habe und verpflichte mich, jedmögliche, die obigen Angaben betreffenden Veränderungen, dem IPHS-Promotionsausschuss unverzüglich mitzuteilen.

02.09.2022	Elena Sildatke
Datum	Unterschrift